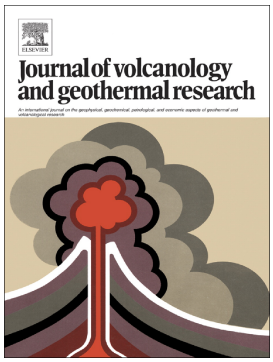

Temporal and spatial variations of CO2 diffuse volcanic degassing on Cuicocha Caldera Lake – Ecuador

Daniel Sierra, Silvana Hidalgo, Marco Almeida, Nicolas Vigide, María Clara Lamberti, Antonio Proaño, Diego F. Narváez

PII: S0377-0273(20)30581-3

DOI: https://doi.org/10.1016/j.jvolgeores.2020.107145

Reference: VOLGEO 107145

To appear in: *Journal of Volcanology and Geothermal Research*

Received date: 21 September 2020

Revised date: 26 November 2020

Accepted date: 29 November 2020

Please cite this article as: D. Sierra, S. Hidalgo, M. Almeida, et al., Temporal and spatial variations of CO2 diffuse volcanic degassing on Cuicocha Caldera Lake – Ecuador, *Journal of Volcanology and Geothermal Research* (2020), https://doi.org/10.1016/j.jvolgeores.2020.107145

Temporal and spatial variations of CO_2 diffuse volcanic degassing on Cuicocha Caldera Lake – Ecuador

AUTHOR'S LIST

1.- Daniel Sierra (Corresponding author)

Instituto Geofísico de la Escuela Politécnica Nacional, Quito-Ecuador.

Instituto de Estudio Andinos "Don Pablo Groeber", UBA-CONICET, Buenos Aires - Argentina.

diserra@igepn.edu.ec

2.- Silvana Hidalgo

Instituto Geofísico de la Escuela Politécnica Nacional, Quito-Ecuador.

shidalgo@igepn.edu.ec

3.- Marco Almeida

Instituto Geofísico de la Escuela Politécnica Nacional, Quito-Ecuador.

malmeida@igepn.edu.ec

4.- Nicolas Vigide

Instituto de Estudio Andinos "Don Pablo Groeber", UBA-CONICET, Buenos Aires - Argentina.

ncvigide@gl.fcen.uba.ar

5.- María Clara Lamberti

Instituto de Estudio Andinos "Don Pablo Groeber", UBA-CONICET, Buenos Aires - Argentina.

mclamberti@gl.fcen.uba.ar

6.- Antonio Proaño

Instituto Geofísico de la Escuela Politécnica Nacional, Quito-Ecuador.

Université Clermont Auvergne, Laboratoire Magmas et Volcans, Clermont Ferrand, France

antoppa18@hotmail.com

7.- Diego F. Narváez

Université Clermont Auvergne, Laboratoire Magmas et Volcans, Clermont Ferrand, France

Departamento de Geología, Escuela Politécnica Nacional, Quito - Ecuador.

diego.narvaez@etu.uca.fr

KEYWORDS

Diffuse degassing

Carbon dioxide

Cuicocha

Cotacachi Cuicocha Volcanic Complex

Crater Lake

ABSTRACT

Cuicocha Caldera is the youngest eruptive center of Cotacachi-Cuicocha Volcanic Complex, located at the north of Ecuador. The caldera contains a lake of 3.95 km^2 surface, and a maximum depth of 148 m. Cuicocha Lake is characterized by the presence of CO_2 gaseous diffuse emissions, perceptible as bubbling zones. Since 2011, CO_2 diffuse flux measurements have been performed in this lake using the accumulation chamber method. The data obtained from twenty surveys were processed by means of the Graphical Statistical Approach and the Sequential Gaussian Simulation. The results reveal that Cuicocha lake has released a total estimated amount of ~400 kt of CO_2 in the period between March 2011 and May 2019, with an average rate of 135 t/day. Furthermore, the spatial and temporal analysis of the data made possible the understanding of the processes occurring in the lake: 1) Lake stratification caused by the seasons seem to favor CO_2 accumulation in the hipolimnion and its posterior releasing. Minimum total flux values of ~50 t/day have been estimated during "warm" stratified periods and maximum flux values of ~170 t/day have been recorded during "cold" overturn periods. Additionally, at least two anomalous degassing episodes were identified in 2012-2013, seemingly associated to changes in the volcanic activity also detected through seismicity. 2) Cuicocha CO_2 degassing seems to be controlled by the existence of diffuse degassing structures at the lake bottom, which correspond to high permeability zones resulting from the intersection between ~NE-SW and ~WNW-ESE oriented structures. We propose a conceptual model to explain the systematic apparition of CO_2 anomalies on specific areas of the lake surface.

1.-Introduction

Volcanic monitoring includes the use of geochemical techniques applied to superficial fluid emissions to understand processes occurring inside the volcanoes (Fischer and Chiodini, 2015). The study of the spatial distribution of CO_2 emissions has become a widespread monitoring tool for volcanologists around the globe in the last two decades (Andrade et al., 2016; Bernard et al., 2004; Cardellini et al., 2003; Hernández et al., 1998; Mazot, 2005; Mazot and Taran, 2009; Viveiros et al., 2010). Several authors have demonstrated an effective application of this method in volcanic monitoring (Melián et al., 2014; Pérez et al., 2006; Rogie et al., 2001) and in the study and identification of structures related to hydrothermal systems (Andrade et al., 2016; Chiodini et al., 2001; Giammanco et al., 1998; Lamberti et al., 2019; Sugisaki et al., 1983).

Cuicocha caldera lake is the youngest eruptive center of the Cotacachi-Cuicocha Volcanic Complex (CCVC), located at the north of Ecuador, South America. Its surface activity is characterized by light gaseous emissions, perceptible as bubbling zones and scattered areas with dead vegetation (Padrón et al., 2008). Cuicocha volcano has been cataloged as potentially active (Almeida et al., 2019; Bernard and Andrade, 2011; Pidgen, 2014; Von Hillebrant, 1989) and it is monitored by the *Instituto Geofísico de la Escuela Politécnica Nacional* (IG-EPN) since 1998.

In 2010, the volcano showed an increase on its seismic activity; small earthquakes (magnitude <4.5, 10-14 km depth)(IGEPN, 2010), some of them felt by inhabitants near the volcano, were registered in the area (Ruiz et al., 2013). Since then, at least eight seismic swarms have been

recorded (IGEPN, 2019, 2018). Although the risk of limnic eruptions is low, the youngness of the caldera and the amount of water forming the caldera lake makes it suitable for a phreatic eruption, as pointed out by Gunkel et al. (2008).

Padrón et al. (2008) mapped the CO_2 diffuse emissions in CCVG for the first time in 2006, using the accumulation chamber method. These authors estimated a total flux of 53.1±2 t/d coming from the lake surface. Later, in 2011, the IG-EPN started periodic diffuse degassing surveys in the lake, incorporating this task to the volcanic monitoring routine. In this work we present the results of nearly a decade of CO_2 diffuse flux measurements. We processed the flux data in order to: (I) map the spatial distribution of the diffuse emissions and quantify the daily amount of CO_2 released from the lake surface; (II) identify the temporary and spatial variations in the CO_2 diffuse emissions; (III) evaluate a possible link between volcanic degassing and tectonic structures; and (IV) discuss the results from a perspective of volcanic monitoring and eruption forecasting.

2.- Tectonics and Geological Setting

Volcanism in the Andean Northern Volcanic Zone (NVZ) results from the subduction of the Nazca oceanic plate beneath the continental South American plate (Guillier et al., 2001; Stern, 2004). At the equatorial latitude, the convergence direction is slightly oblique with respect to the continental margin (Figure 1-A). The aseismic Ridge of Carnegie, originated from the Galápagos hot spot, subducts below Ecuador, generating a transpressive regime (Freymueller et al., 1993; Graindorge et al., 2004; Yepes et al., 2016). The Ecuadorian Andes, have an extension of ~650 km (Hall et al., 2008) and comprise at least 84 volcanoes and volcanic complexes (Figure 1-A) (Bernard and Andrade, 2011). Five of these volcanoes erupted in the last 3 decades: Tungurahua (Arellano et al., 2008; Hidalgo et al., 2015), Pichincha (Garcia-Aristizabal et al., 2007), Cotopaxi (Bernard et al., 2016; Gaunt et al., 2016; Hidalgo et al., 2018), Reventador (Samaniego et al., 2008) and Sangay (Monzier et al., 1999).

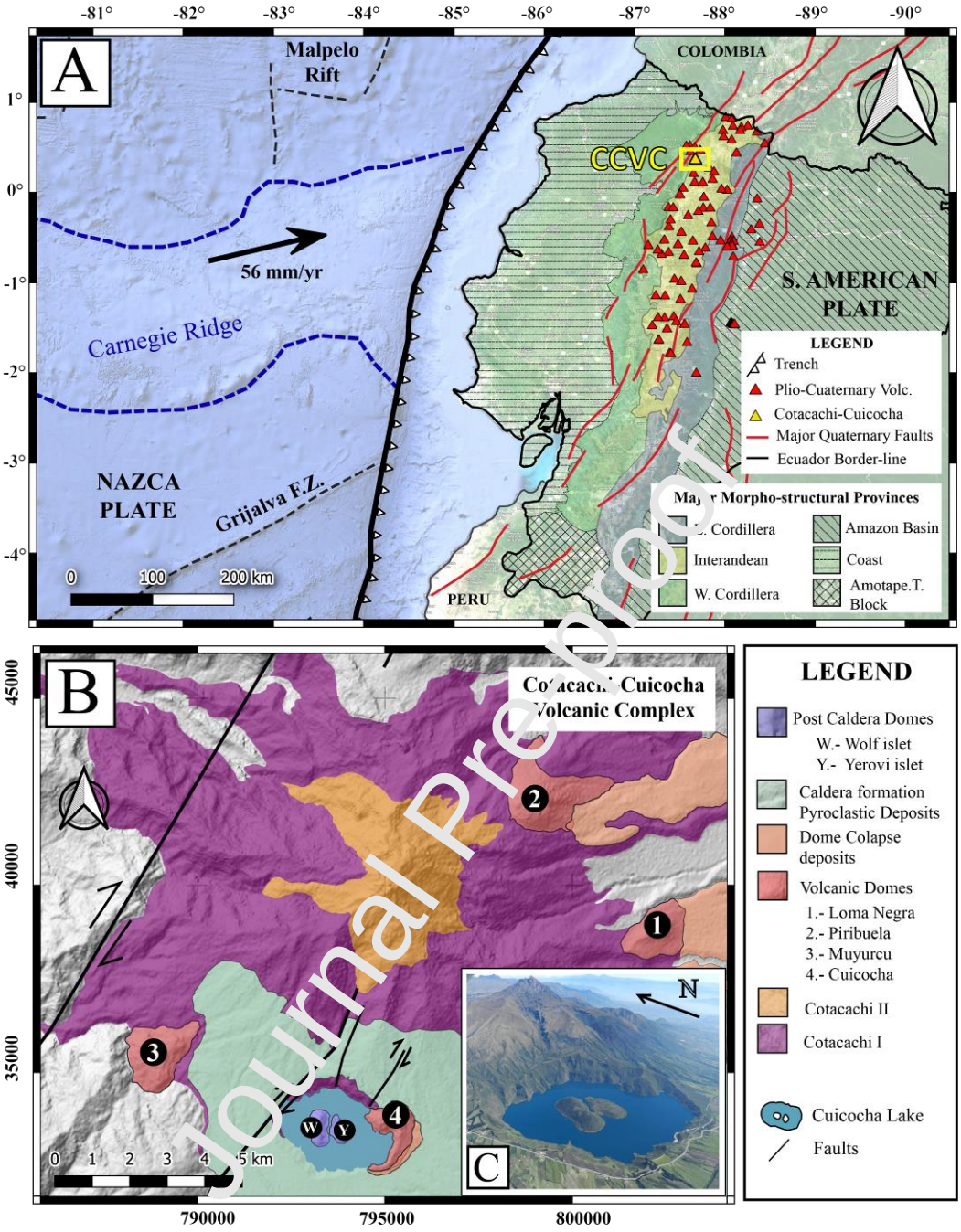

Figure 1.- A) Geodynamical setting of the Ecuadorian Arc. Base Map (openstreetmap.org). Geographic Coordinates - WG S84. Regional Geology (Eguez and Albán, 2017). Plio- Quaternary Volcanoes (Bernard and Andrade, 2011). Major Faults (Eguez et al., 2003). Geodynamical settings (Gutscher et al., 1999). Plate convergence rate (Nocquet et al., 2009). B) Simplified Geology for Cotacachi-Cuicocha Volcanic Complex (Almeida, 2016). UTM Coordinates WGS84-17N. C) Aerial view of the Cotacachi Cuicocha Volcanic Complex from the SW. Photography: M. Almeida.

Many authors have suggested that the old continental accretion sutures and other tectonic structures oriented ~N-S (Alvarado, 2012; Guillier et al., 2001; Lavenu, 1995; Soulas, 1991) played an important role in the emplacement of some Ecuadorian volcanoes (e.g. Papale and Rosi, 1993; Samaniego et al., 2012; Tibaldi, 2005). These volcanoes are arranged forming alignments (Hall et al., 2008; Hall and Beate, 1991) which also exhibit systematic compositional variations from W to E. Based on these constrains, 3 volcanic domains have been defined: the Volcanic Front, the Main arc, and the Back arc (Bourdon et al., 2003; Hidalgo et al., 2012;

Samaniego et al., 2002). The nature of the basement of these domains is variable including the oceanic basalts, dioritic intrusions and pyroclasts of Western Cordilllera (Hughes and Pilatasig, 2002; Vallejo et al., 2009), the metamorphic, igneous and metasedimentary rocks of the Eastern Cordillera (Aspden and Litherland, 1992; Pratt et al., 2005), and the volcanic origin units of the Interandean Valley (Hall and Beate, 1991) (Figure 1-A).

Cotacachi-Cuicocha Volcanic Complex (CCVC) is located ~70 Km north of Quito, the capital city of Ecuador; comprised within the Volcanic Front, it covers an area of ~260 km^2 (Figure 1-B) and it is surrounded by important urban centers like Cotacachi (pop. 8800) and Quiroga (pop. 3200). The eruptive history of CCVC includes numerous stages, which resulted in different morphological expressions on the surface: a central stratovolcano surrounded by "satellite" domes and a volcanic caldera (Almeida, 2016; Almeida et al., 2019). The emplacement of the older main edifice (Cotacachi Volcano) started ~160 ka with two major stratigraphic units: Cotacachi-I and later Cotacachi-II (basaltic-andesite/andesite lava successions) (Almeida, 2016). Later, the construction of the "satellite" domes occurred: Muyurcu, Loma Negra, Piribuela and Cuicocha (chronologically ordered). Around 3000 B.P., explosive eruptive episodes destroyed the Cuicocha dome and formed a volcanic caldera (Von Hillebrant, 1989). The caldera formation was accompanied by the emission of large volumes of pyroclastic products, whose deposits are widely spread covering vast areas, specially to the SE of the caldera (Almeida, 2016; Pidgen, 2014; Von Hillebrant, 1989). The last evidence of eruptive activity corresponds to the extrusion of intra-caldera acid andesitic domes distributed in the Wolf and Yerovi islets (0,44km^2 and 0,27km^2, respectively) (Almeida, 2016; Almeida et al., 2019; Padrón et al., 2008).

Furthermore, the local tectonic settings are associated with Huayrapungo and Billecocha fault systems (Eguez and Yepes, 1993), which comprise a set of ~NE-SW faults coupled to the Major Dextral System (MDS) of the Ecuadorian Andes (Ego et al., 1996; Eguez et al., 2003; Soulas, 1991). The MDS is responsible for the NE-ward displacement of the North Andean Sliver (Alvarado, 2012; Pennington, 1981). The stress state of the region is characterized by a maximum horizontal compressive axis oriented N80° (determined ~20 km NE from the CCVC) (Cordova, 2013). The morphology and the structural features of CCVC show the influence of these main fault systems (Almeida, 2016).

Nowadays, the Cuicocha caldera has a lake, its origin has been attributed to the deglaciation of the main edifice in the Pleistocene, rain and hydrothermalism (Gunkel and Beulker, 2009). The resultant lake is separated into two different basins with a maximum deep of 148 m at the east and 78 m to the west (Gunkel and Beulker, 2009; Padrón et al., 2008). The lake has no superficial outflow, but ravines formed at the eastern side of the caldera suggest the existence of subsurface outflows. Only two small cascades act as inflow, in addition to moderate precipitations occurring throughout the years. The lake reaches an altitude of 3060 m.a.s.l., the water covers a surface of 3.95 km^2 and has an estimated volume of 0,28 km^3 (Gunkel and Beulker, 2009).

3.-Methods

3.1- Carbon dioxide diffuse degassing

A total of 20 CO_2 flux measurement surveys were performed on the caldera lake surface, carried out by IG-EPN staff as part of the routine monitoring activities. The surveys were randomly distributed in time (based on resources and logistic facilities) between March 2011

and May 2019, with a rate of 1 to 4 campaigns per year (see **Error! Reference source not found.**).

Each campaign consisted of ~100 measurements (**Error! Reference source not found.**), forming almost-regular grids on intervals of 200-300 m (Appendix I), covering the total area of the lake. The sampling points were geolocated using a Garmin handheld GPS. The measurements were performed using the accumulation chamber method (Chiodini et al., 1998; Parkinson, 1981), originally designed for soil emissions but also applicable for water surfaces (eg. Bernard et al., 2004; Mazot and Taran, 2009; Padrón et al., 2008). The implemented instrument was a portable West Systems flowmeter which is equipped with an infrared spectrometer (LICOR Li-800) operating in the range 0–20,000 ppm of CO_2, an accumulation B-type chamber (volume 0.006186 m^3) attached to a flotation device, and a palm-PC/tablet connected via Bluetooth which is used as data logger (West Systems, 2019). The uncertainty of the measurements has been estimated to be around 10% for CO_2 fluxes between 10 and 10,000 g m^{-2} d^{-1} (Chiodini et al., 1998), although this number can be larger if fluxes are low (up to 24% for fluxes of 5.7 g m^{-2} d^{-1}) (Carapezza and Granieri, 2004). Teams of 2-3 operators performed the flux measurements sailing into the lake in a boat, each survey lasted approximately 3 working days.

Since 2015, water temperature was taken at each measurement site. This variable was measured at a depth of 0.3 m by means of a Thermo Scientific Orion-5 multi-parametric device, equipped with a temperature cell model #013010MD designed for an operational range from -5 to 105 °C, displaying a resolution of 0.1 °C.

In order to understand the origin of the CO_2, the flux data were analyzed with the Graphical Statistical Approach (GSA) method. This probability plot technique is based on the partitioning of complex multimodal distributions into different log-normal populations (Sinclair, 1974; Tennant and White, 1959). It allows to distinguish different possible sources contributing to the CO_2 flux; for example, the background emissions and the anomalies (generally attributed to biological and volcanic sources respectively). This method can be also used to estimate the total CO_2 emitted in a particular area (Cardellini et al., 2003; Chiodini et al., 1998; Viveiros et al., 2010). It is important to mention that the reliability of the CO_2 output obtained from the GSA could be affected by operator bias during the partitioning procedure (Cardellini et al., 2003); another drawback is that the GSA does not consider the spatial distribution of the measurements, implicitly assuming a homogeneous sampling density (Cardellini et al., 2017).

The datasets were modeled using the least possible amount of log-populations, with a maximum of 4 (Chiodini et al., 1998). Validity of models was checked through calculation of ideal combinations of partitioned populations (Appendix II), until a satisfactory agreement between ideal mixtures and real data was obtained (Chiodini et al., 1998). The mean and the 95% confidence interval of the mean were computed with the Sichel t-estimator (David, 1977).

For CO_2 flux mapping, we used the Sequential Gaussian Simulation (SGS) (Cardellini et al., 2003). This method presents advantages over the traditional interpolation methods (e.g. regular kriging), since it provides a set of equiprobable results to occur instead of producing a single representation that yields the minimum error variance at each location. The ensemble of these realizations is an approximate representation of the single, but unknown reality (Cardellini et al., 2003; Rautman and Istok, 1996). For every single campaign data set, we computed and modeled the experimental variograms of the normal scores (Appendix III). Then, the models were used in the SGS procedure to create 200 simulations of the normal scores, using the Sgsim program (Deutsch and Journel, 1998); setting a 25 m cell size same as

Padrón et al. (2008). The simulated normal scores were back-transformed to original data units, applying the inverse of the normal score transform. The mean flux value and the variance were calculated at every single cell and assumed as characteristic values (Cardellini et al., 2003). Finally, the total CO_2 output was computed by summing up the products of the simulated value of each grid cell multiplied by the cell surface.

3.2- Analysis of the structural control

The structural analysis includes bibliographic data from the "Database and Map of Quaternary faults" (Eguez et al., 2003), the local Geological Map (INIGEMM - 1:50 000; Andrade and Guarderas, 2017), local volcanological studies in CCVC (Almeida, 2016), and the bathymetric data of the lake (Gunkel and Beulker, 2009).

The main morpho-structural lineaments were manually interpreted, over an area of 200 km^2, using a 12.5 m digital elevation models (DEMs) from ALOS Palsar RTC (https://asf.alaska.edu/) to characterize the geometric structural configuration of the study area. Lineaments are defined as linear observable features on the earth's surface which differ distinctively from the patterns of adjacent features and presumably reflect shallow depth phenomena (O'leary et al., 1976). The directions of the identified lineaments were statistically analyzed to identify preferential orientations (Mardia, 1972) and represented as rose diagrams using "Angle Histogram", an open source toolbox written in MATLAB (Trauth et al., 2007). This geometrical analysis offers suitable approach for identifying subtle evidence of structural control and possible damage zones, which could be related to the diffuse degassing.

Additionally, in order to recognize the CO_2 anomalous flux areas, potentially linked to diffuse degassing structures (DDS), we followed the criteria presented by Chiodini et al. (2001) and Lamberti et al. (2019). It is important to note that the areas with anomalous flows do not necessarily occur at the same place in every survey, so we identified areas where the anomalies are repeated over time. Using Quantum-GIS (QGIS Development team, 2015), the anomalous and non-anomalous degassing zones were manually delimited and transformed in matrices of ones and zeros; the GSA results were used as guidelines to define the threshold background/anomaly in every case. All the matrices were summed, and the resultant pixel values were normalized to percentage. Afterwards, they were plotted in a single "anomaly map" (25 m grid cell) showing the areas where a CO_2 anomalous value is most probable to occur in the Cuicocha lake.

Considering that lake-bottom structures cannot be directly observed due to the water body, inland tectonic features were extrapolated, as it was performed in the study of Furnas lake, Azores (Andrade et al. 2016). Finally, a conceptual model showing the possible relationship between CO_2 anomalies and subaquatic DDS was constructed.

4.-Results

4.1-Surface water temperature

During the 2015-2019 period, when water temperature measurements were performed, no substantial variations were observed in this parameter. Only minor seasonal changes were registered with the surface temperature of the lake showing a range between 15 and 18 °C. These small variations are attributed to the dry and rainy seasons in the area and to the sun light incidence throughout the day. In every survey, the temperature of the lake tends to be very stable without significant temperature anomalies, even in the areas characterized by anomalous CO_2 fluxes.

In 2009, Gunkel and Beulker reported the existence of a hydrothermal inflow from the bottom. These authors characterize this inflow as a warm (23-26 °C), ion enriched (2880µS c/m) water detected in some specific points within the lake. However, due to the low flow, this ion enriched water rapidly mixes within the lake water and these manifestations are very difficult to observe from the surface, where the temperature and conductivity show the ranges of a natural lake (Gunkel et al., 2006).

4.2- CO_2 diffuse degassing

The CO_2 flux measurements are distributed in a range of values from 0.69 g m^{-2} d^{-1} up to 631.4 g $m^{-2}d^{-1}$ (**Error! Reference source not found.**). All 1923 CO_2 individual flux measurements collected from 2011 to 2019, have been homogeneously processed. The application of the GSA method allowed the modeling of our datasets as a combination of log-normal populations.
The results of GSA application have been summarized in Figure 2, the logarithmic probability plot shows how each survey plot has its own particular distribution. Most of the curves for the period 2011-2019 present an almost flat shape with discrete inflection points in the central part and more pronounced breaks in the tails. All the datasets were modeled combining up to 4 populations (Appendix II). Populations A were used to model the upper tail values, populations B and C model the central data (the bulk) and D populations were used to model the points at the lower tails (Figure 2). Populations A and B include the "high flux" values, displaying mean values generally rounding 20-70 g m^{-2} d^{-1}. On the other hand, C and D populations comprise the "low flux" values with mean values among 5-40 $m^{-2}d^{-1}$ (**Error! Reference source not found.**).

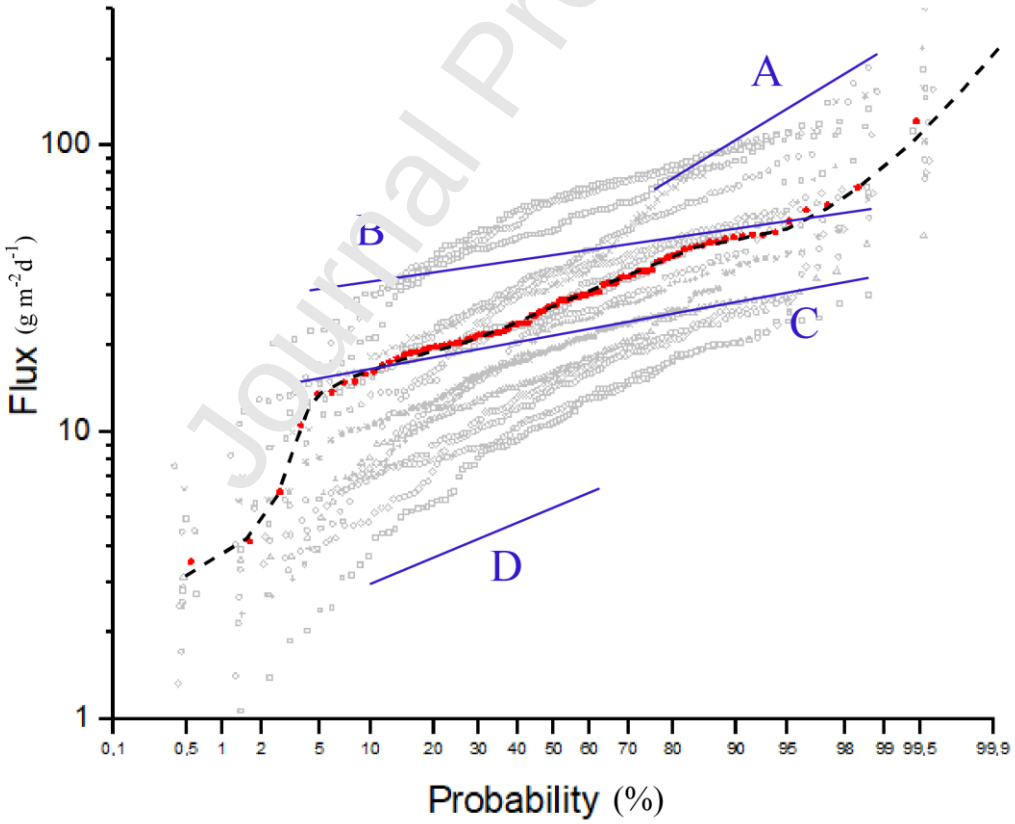

Figure 2.- Log probability plot of the CO_2 fluxes. Grey dots show log CO_2 flux data statistical distribution for all the surveys. The Mar-2014 dataset is shown as an example with red dots; the partitioned populations using GSA method are shown with blue lines (A and B for High Flow, C and D for Low Flow populations). The theoretical distribution resulting from the combination of the HF and LF populations are shown with the black dashed line, the correspondent proportions are 8 and 32 % for HF and 55 and 4.5 % for LF.

To characterize the spatial distribution of CO_2 fluxes, data have been processed with SGS to produce 20 CO_2 flux distribution maps. The resulting maps for each survey are shown in Figure 3. The Cuicocha lake exhibits diverse degassing patterns over time. Some maps show scattered CO_2 flux anomalies within the lake surface, in the zones corresponding to the deeper part of the eastern basin, the northern corner of Yerovi islet (the bubbling zone) and the NW corner of the lake (e.g. Mar 2014, Apr 2017, Feb 2018, Jan 2019). On the other hand, other maps show practically regular CO_2 flux values over the entire surface of the lake. These regular values can be either low (e.g. May 2018, May 2019) or high (e.g. Aug 2017, Sep 2012). The systematic presence of some anomalies suggesting the existence of DDS feeding the Cuicocha caldera lake with deep-sourced CO_2 will be discussed later.

The total daily flux was also estimated by mean of GSA and the SGS methods. Both procedures reached remarkably similar results (**Error! Reference source not found.**). The results obtained by both methods in no case exceed 4% difference, supporting the validity of both estimations. The total daily fluxes range ~50-250 t/d, with the highest flux values occurring in 2012-2013.

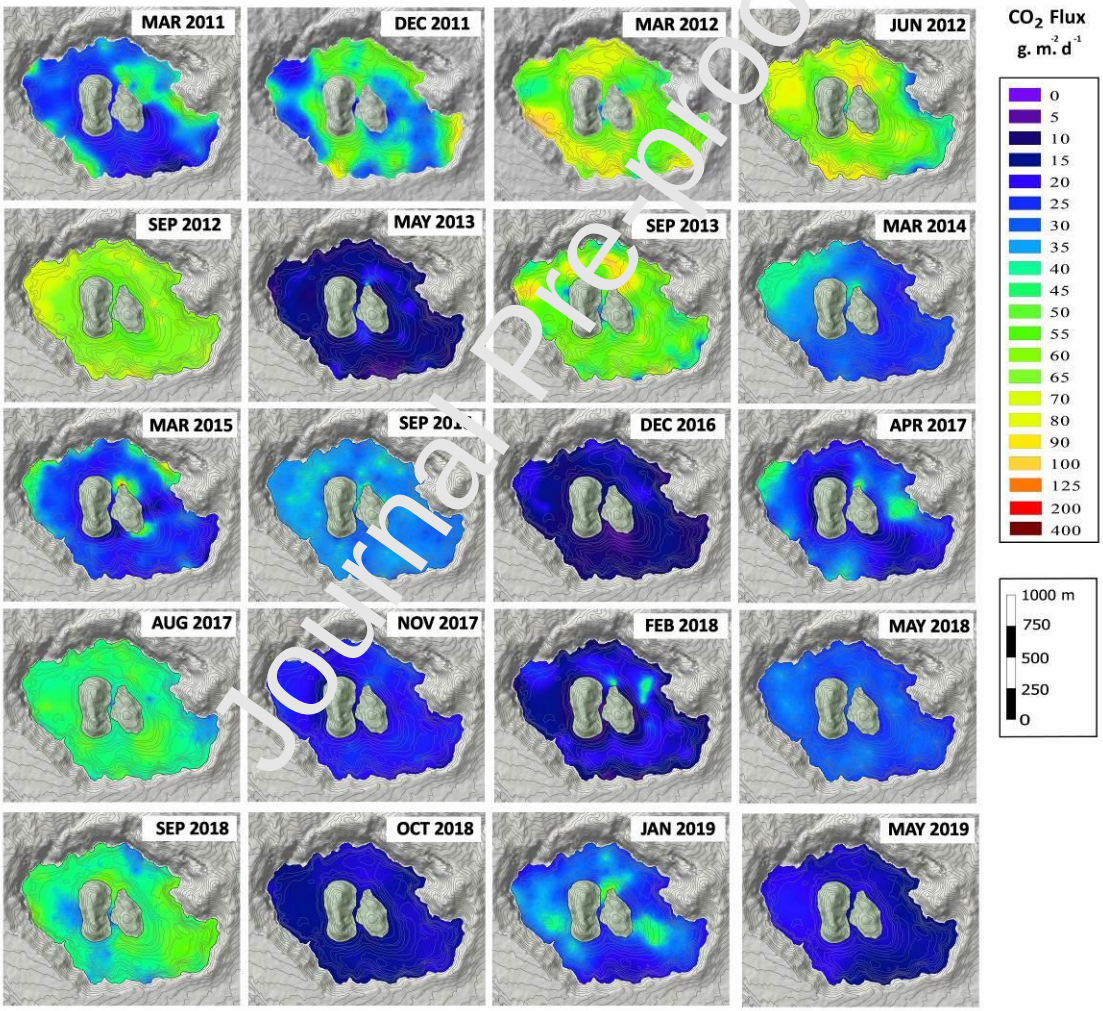

Figure 3.- CO_2 diffuse degassing in Cuicocha lake during 2011-2019 period. The maps show the flux expressed in g m^{-2} d^{-1} with a grid-cell of 25 m. The maps were plotted using the software QGIS (QGIS Development team, 2015). The lake border and 20 m contour lines were extracted from a 12.5m resolution DEM. Bathymetric contour lines 20 m (Gunkel and Beulker, 2009) have also been collocated for reference.

4.3- Structural Features

The local major structures were compiled in a map using QGis over a hillshade-layer based on a 12.5 m DEM (Figure 4-A). The major Quaternary faults present in the area (red lines in Figure

4-A) show lengths greater than 20 km and present a ~NE-SW orientation. These major faults are part of the Billecocha and Huayrapungo fault systems (Eguez et al., 2003; Soulas, 1991). Structural boundaries between the Cretaceous and Paleocene geological units forming the Western Cordillera (blue lines) are also characterized as long traces with ~NE orientation. Their movement is also coupled to the kinematics of the MDS (Andrade and Guarderas, 2017). Additionally, minor local faults (orange lines in Figure 4) have been identified over the southern flank of Cotacachi (Almeida, 2016). Their traces have lengths are of about ~2 km and reach the northern border-wall of the Cuicocha Lake.

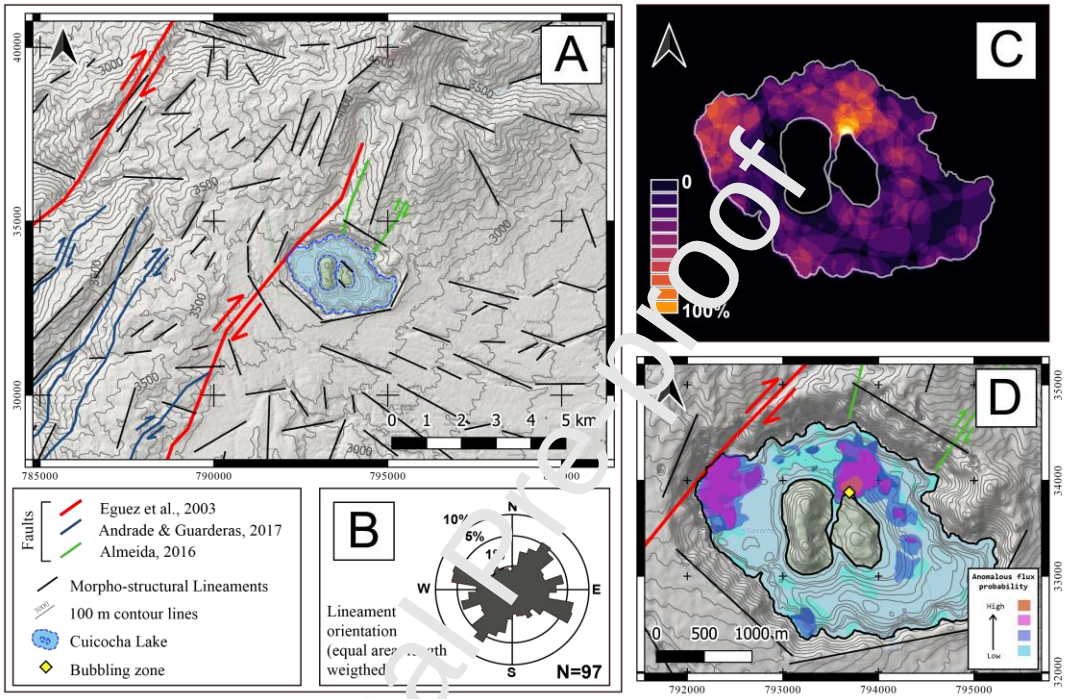

Figure 4.- A) Morpho Structural Analysis of the region. B) Rose Diagram for morpho-structural lineaments length weighted C) Heat map based on the compilation of CO_2 anomalous zones for the 20 surveys, the color scale shows the areas where an anomaly is most probable to occur. D) Zoom to figure A at Cuicocha Lake including the results of the compilation of anomalous zones showed on C. The probability of an anomalous flow is shown in 4 categories with thresholds at 30, 40, 50 and 80%.

Moreover, almost a hundred of morpho-structural lineaments were identified in the area around the lake (black lines, Figure 4-A). The rose diagram on Figure 4-B shows the statistics of the lineaments azimuths (length-weighted with a bin of 10°). Two main trends could be observed ~WNW-ESE and ~NE-SW-orientated; also, a secondary trend ~ENE-WSW was recognized. These trends are not arbitrary, the ~NE-SW oriented lineaments seem to be parallel to the local and regional major faults; while ~NW-SE are parallel to other minor structural features like fold axes and faults, recognized by several authors (Andrade and Guarderas, 2017; Ujueta, 2001; Yepes et al., 2016). Finally ~ENE-WSW lineaments seem to be parallel to the plate convergence direction (Nocquet et al., 2009) and to the horizontal compressive axis calculated for this zone (Cordova, 2013).

These evidences suggest a possible structural control in Cuicocha Caldera. In fact, some of the Caldera border-walls have very steep slopes (40– 90°) displaying quite straight traces parallel to both main lineament trends. The eastern basin lake-bottom and some of the borders of Yerovi Dome are also coincident with those orientations (Figure 4-D).

Figure 4-C shows the compilation of the anomalies registered for the 20 surveys of CO_2 diffuse degassing normalized to percentage. The 'hotspots' for CO_2 anomalies occur in the northern corner of the Yerovi Dome, the area corresponding to the bottom of the eastern basin (NW-aligned), and the northwest and south corners of the lake. (Figure 4-D). These anomalous zones recognized in the lake surface and its possible relation with the tectonic features will be discussed in the next section.

5.- Discussion

5.1 The sources for CO_2 emissions

In volcanic environments, the presence of several log-normal populations that model CO_2 flux polymodal distribution, (discriminated by means of the GSA method), can be interpreted as the existence of different gas sources. It can also be interpreted as the occurrence of different mechanisms of gas transport, different permeability in the soils/rocks, etc. (Cardellini et al., 2017). In the same way, the absence of a clear polymodal distribution could be the result of the presence of a widespread low level degassing of deeply derived CO_2 linked to the several degassing structures active in the area (Cardellini et al., 2003).

The CO_2 flux datasets were modeled up to 4 log-normal populations. In most of the cases two of them (C and D) likely correspond to the "background", and the other two populations (A and B) describe the high flux probably coming from a deep source. Furthermore, Padrón et al. (2008) already applied the GSA method in Cuicocha Lake achieving similar results, using the techniques proposed by Sinclair (1974) and Woodcworth (1971). Padrón et al. (2008) interpreted the existence of two populations: one of low flux (mean 4.1 g $m^{-2}d^{-1}$), and other of high flux (mean 17.3 g $m^{-2}d^{-1}$), presenting proportions of the whole data set of 29 % and 71 % respectively.

Degassing via bubble plume and by diffusion through the lake can explain the different ranges in flux values (Mazot et al., 2014). The high mean CO_2 flux values could be indicative of feeding by CO_2 up-rising from the underlying hydrothermal system (e.g. Cardellini et al., 2017, 2003; Chiodini et al., 1998). High mean populations could also be attributed to the presence of sub-lacustrine vents discharging CO_2 into the lake (Mazot et al., 2014). In the same way, populations with atypically very-high means (corresponding to anomalous points in the upper tails) present in some data sets, could correspond to areas or places where the CO_2 inflow has a very direct ascent path or comes from very shallow degassing zones. An example could be the bubbling zone located in the northern corner of Yerovi islet, where isotopic analysis have confirmed the presence of deep origin CO_2 (Inguaggiato et al., 2010).

However, the interpretation of the "low flux" populations could be more complex. It is widely accepted that the origin of these populations could be attributed to biologic activity. The mean value for biogenic CO_2 flux from a wide variety of ecosystems ranges from 0.2 g $m^{-2}d^{-1}$ to 21 g $m^{-2}d^{-1}$ (Viveiros et al., 2010), however more recent studies reveal the biogenic sources could reach fluxes up to 45 g $m^{-2}d^{-1}$ (Viveiros et al., 2020). In 2014, (Mazot et al., 2014) proposed a model to calculate the flux originating from diffusion at air-water boundary (Liss and Slater, 1974) for their studies in Lake Rotomahana, New Zealand; this model considers a thin film between the water and the atmosphere, and uses an empirical equation similar to Fick's Law (McGillis and Wanninkhof, 2006). The gas transfer velocity could be calculated as a function of wind-speed and water temperature (Mazot et al., 2014). We used the same equations with a temperature of 17 °C and average wind speed at lake level of 9 km/h (wind speed was estimated based on data registered at the nearest Meteorological Station "Inguincho"; 2011-2019 INAMHI). Thus, the CO_2 flux by diffusion to the atmosphere must be around 24 g $m^{2}d^{-1}$ for Cuicocha Lake.

Additionally, the presence of anomalous points in the lower tails results in populations with very low means. In volcanic lake environments it has been suggested that populations presenting very low means (~1 g $m^{-2}d^{-1}$) could be attributed to the absorption of CO_2 via biological activity of algae thereby decreasing the CO_2 diffusion to the atmosphere (Mazot et al., 2014).

Based on the GSA calculations (**Error! Reference source not found.**) and considering the limits established for the biological activity proposed in the literature, we suggest that the threshold between the fluxes coming from volcanic origin emissions and those corresponding to the "background" (biological and other non-defined sources) must be around 20-30 g $m^{-2}d^{-1}$. However, this assumption is not conclusive, the application of combined methods including gas isotopic analysis (Bini et al., 2020) is required to get a better understanding of possible sources contributing to diffuse degassing in Cuicocha lake and their relative proportions.

5.2 Temporal variations of CO_2 degassing

- The effect of the climatic conditions

Due to the geographic position (near lat.0°), the oceanic currents, and the presence of the Andes, the weather in Ecuador has a particular behavior characterized by non-well defined seasons (Bendix and Lauer, 1992). The regional climate is determined by regular and intense air temperature oscillation (Gunkel, 2000). For the zone of Cotacachi/Cuicocha, the mean ambient temperature is ~15 °C, with a slight annual variation (less than 1°C). Nevertheless, for an ordinary day the thermal amplitude is relatively wide, oscillating between 9 ° and 22° C. In average, the coldest and also the driest month of the year is July (climate.org, 1982 - 2012).

The climate causes important effects over the lake dynamics. Cuicocha has been described as a weakly thermal stratified lake (Gunkel and Beulker, 2009). From September to May, a high solar radiation input heating the surface of the water favors the thermal stratification (Gunkel, 2000). During that period, the epilimnion stretches down to 40 m (Gunkel and Beulker, 2009). From June to August, the strong winds of the dry season (Gunkel, 2000), create a "cold period", the temperature of the water body drops, and an overturn process occurs in the lake (Gunkel and Beulker, 2009).

Carbon dioxide is regularly released through Cuicocha Lake all year long (Figure 5). However, some peak discharges have been registered in Jun 2012, Sep 2012, Sep 2013, Sep 2016, Aug 2017 and Sep 2018 (Figure 5-A). All the CO_2 flux peaks seem to occur, during or immediately after the "overturn months"; on the other hand, the lower values seem to occur out of the overturn periods. Additionally, if it is compared with water temperature (available from 2015-2019 only), CO_2 peaks show a good inverse correlation (Figure 5-A).

As suggested by Padrón et al. (2008), during the stratified periods, no convective mechanisms are supposed to occur. Therefore, during these periods hydrothermal CO_2 could remain stored in the depths of the lake. On the other hand, during overturn periods (due to the water cooling) the stratification disappears and a monomictic circulation reduces the accumulation of CO_2 in the deep, favoring a maximum release at the surface (Gunkel et al., 2008; Gunkel and Beulker, 2009; Padrón et al., 2008).

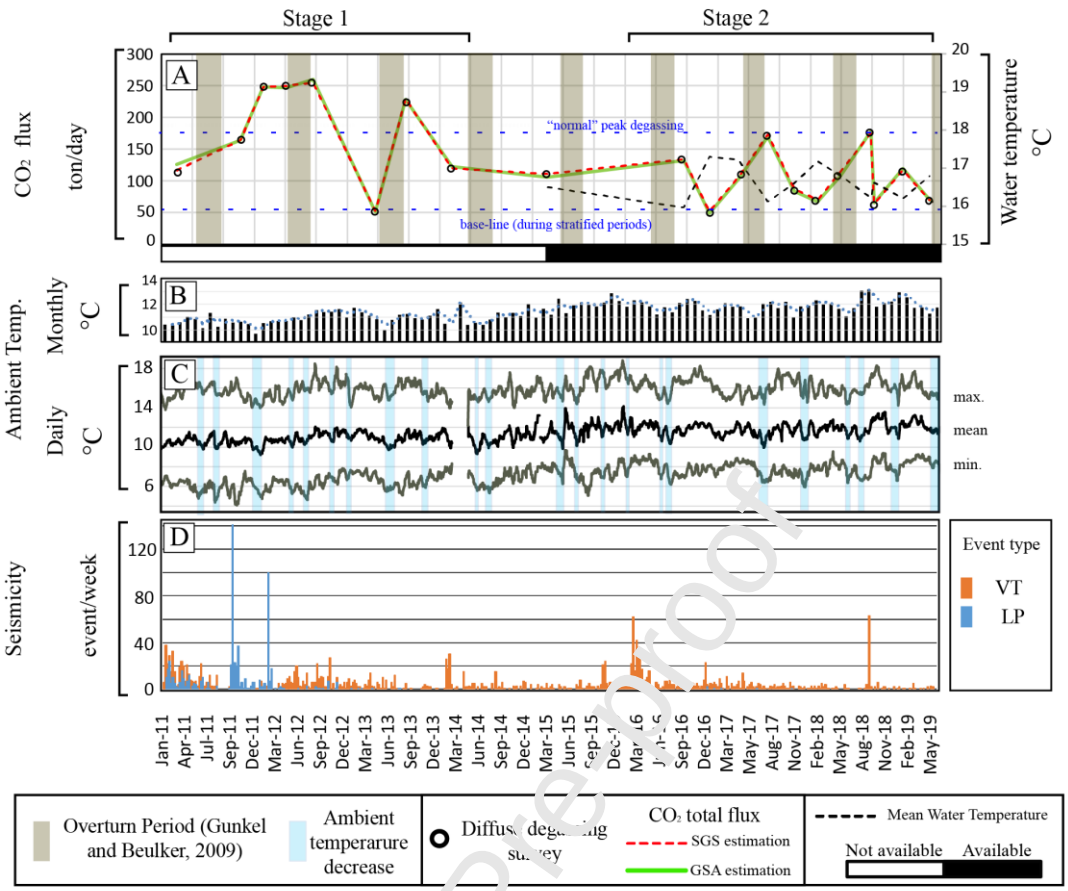

Figure 5.- A) Left Y axis shows total CO_2 flux estimations using SGS and GSA (see methods), Right Y Axis shows water temperature when available. Lake overturn-periods (Gunkel and Beulker, 2009) are highlighted in gray. B) Ambient temperature, monthly average Variation. C) Daily Temperature Values (Max, Mean and Min) softened with a 15-day moving average. Systematic decreases on daily temperature have been highlighted in light-blue. Weather data from: Inguincho Meteorological Station (INAMHI), located 5km SW from CCVC. D) Seismic event count: Volcano Tectonic (VT) and Long Period (LP) (IG-EPN).

Another issue to consider is that the water stratification in Cuicocha has been suggested to be unstable even in the warmer seasons (Gunkel and Beulker, 2009). The slight temperature variations between surface and deep waters, added to the low temperatures recorded at night, could produce dimictic (Gunkel and Beulker, 2009). To establish a comparison with local climatic patterns, the data for the nearest climatic station provided by the Ecuadorian National Weather Service (INAMHI) has been plotted on Figure 5-B, showing the monthly average. Also, Figure 5-C shows the daily maximum, mean and minimum ambient temperatures. The periods when temperature drops occur, are highlighted with a blue background since they could have caused monomictic circulation, leading to an increase in the CO_2 emission rate.

In the period between 2011-2016, coincidences between emission peaks and overturn periods are observed, but the sampling rate is lower (sometimes 1-2 surveys/year). The entire spectrum of temporary variation is not easy to observe due to this lack of data. On the other hand, the surveys performed in 2017-2019 have a higher sampling rate (3-4 surveys/year). The curve on Figure 5-A has an oscillatory repetitive pattern with almost the same peak and bottom values. This pattern could be consistent with the idea of CO_2 flux fluctuations caused by seasonal variations.

- Changes in volcanic activity

Some of the highest estimations for total CO_2 outputs (recorded in 2012-2013) are almost 4 to 5 times higher than the base-line values (ranging ~50-60 t/d; Figure 5) and significantly higher than the 2017-2019 peak values (Figure 5). The question is whether the climatic cycles affecting the lake could be responsible for those differences in the CO_2 outflow or not. This kind of variations might not correspond to a climatic variation only, but could also be a consequence of deep origin processes probably associated to the hydrothermal system.

Temporal variations in CO_2 fluxes can be related to changes in the volcanic activity and may be important for volcanic monitoring and risk mitigation (Hernández et al., 2001; Notsu et al., 2005). Figure 5 shows a comparison in a temporary series between A) the CO_2 total flux of Cuicocha with D) VT and LP events number. Despite of the volcanic origin of the CO_2, there is no clear correlation between diffuse emissions and seismicity. The highest peaks recorded in VT events (generally associated to rock fracture) do not seem to be accompanied by major degassing episodes; for LP events (generally associated to the movement of fluids inside the volcanic edifice), the correlation appears to be poor. However, it is remarkable that the highest peaks recorded for CO_2 total emissions in the entire time series occur during and after episodes of high LP occurrence (2011-2012), and simultaneously to the seismic swarms of Mar 2012 and Oct 2012 (Hidalgo et al., 2014; IGEPN 2019). On the other hand, surveys corresponding to 2014-2019 (where the total fluxes are lower) occur in a time interval characterized by a relative absence of LP events (Figure 5-A and -D).

The timescale presented in this work could be divided in two stages: 1) Pre-2014, when degassing shows anomalous peaks, also characterized by observed anomalies in seismicity with an increase in the number of LP events; 2) Post-2014, when the occurrence of LP events is practically null and the VT seismicity continues. For this second stage, the diffuse degassing peaks are lower. The sampling rate also increases, allowing the observation of repetitive cycles more consistent with seasonal variations.

5.3 Degassing Structures

Almeida (2016) suggested that the morphology of the CCVC is affected by regional faults coupled with the MDS of the Ecuadorian Andes. The Cuicocha caldera border also seems to respond to the regional tectonics, showing a parallelism with the major trends for morpho-tectonic lineaments of the area. A very superficial interpretation, based on morphological expressions, as well as the control of tectonic structures in the area; suggest that pre-existing fractures/faults aligned ~NE-SW and ~WNW-ESE, could have played an important role in the evolution of the volcanic complex like in the caldera formation and/or the subsequent dome emplacements.

Additionally, some of the anomalies in CO_2 flux show a characteristic alignment and location, which are repeated over time (Figure 4-C); similar alignments had been previously reported by Padrón et al., (2008). Those findings suggest the existence of DDS in the lake bottom responsible of the CO_2 emission. It is widely accepted that the intersections zones between cross-cutting structures may cause fracturing and reopening of fluid conducts (Curewitz and Karson, 1997; Martel and Boger, 1998; Sibson and Rowland, 2003), establishing vertical/subvertical high-permeability channels. Tectonic structures similar to those responsible of the caldera shape and dome emplacement, and their intersections could generate high permeability damage zones suitable for CO_2 releasing. Making inferences and extrapolations from the structures observed inland, we present a conceptual model which

successfully resolves the presence of sub-lacustrine diffuse degassing structures where CO_2 anomalies have been observed through almost a decade (Figure 6).

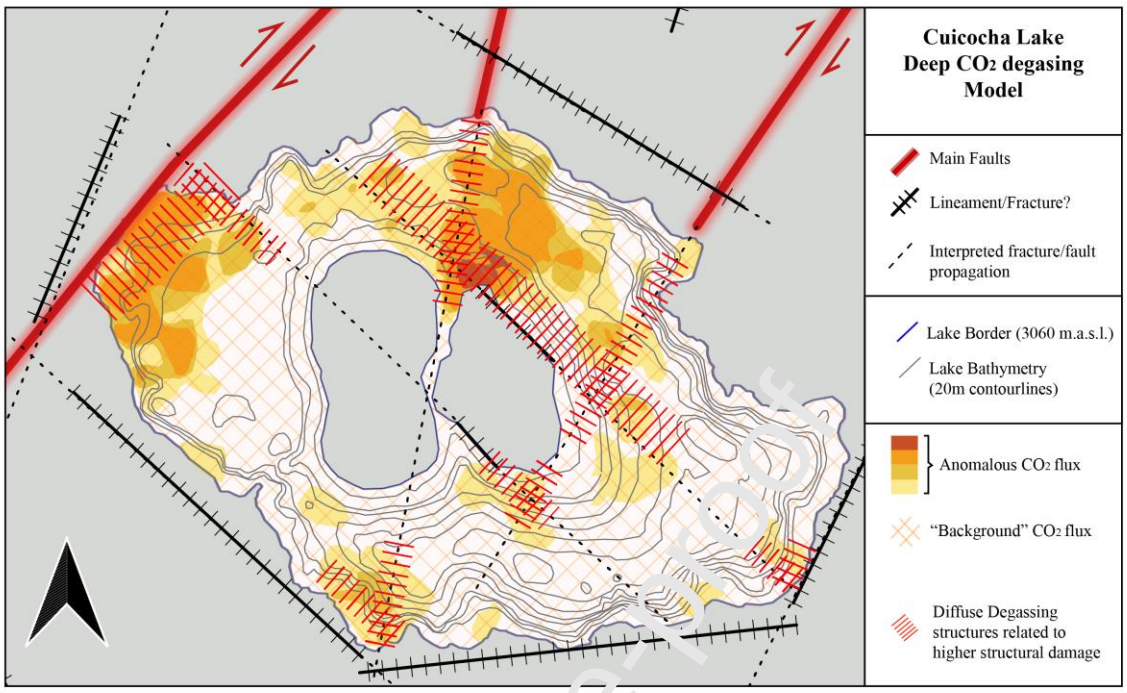

Figure 6.- Conceptual model of the structural scenario explaining the deep CO_2 release at Cuicocha Lake.

This model well explains the presence of CO_2 flux anomalous zones in the lake, but some of the maps presented on Figure 3 present fairly uniform spatial CO_2 distributions; where no punctual anomalies are easily identifiable (e.g. Aug 2017 with "high" generalized values and May 2019 with "low" generalized values). It is unlikely to presume that in the periods in which the lake surface releases gas homogeneously, the entire lake floor releases CO_2 homogeneously as well. These regular distributions, observable in some maps, must be caused by gas diffusion in the water body. Additionally, the storage of CO_2 in the hipolimnion during stratified periods with the subsequent release at overturn could facilitate in some occasions a fairly homogeneous degassing through the water-atmosphere interface.

5.4 CO_2 Emissions to the Atmosphere

Estimating the quantity of CO_2 diffusively emitted from the Earth's surface has important implications for volcanic surveillance and global atmospheric CO_2 budgets (Bini et al., 2020; Fischer and Aiuppa, 2020; Werner et al., 2019). The total CO_2 flux curve presented on Figure 5-A was integrated to estimate the accumulated CO_2 emission. During the time the surveys lasted (8.13 years), the volcano emitted ~400 kt of CO_2, with an average rate of 49.3 kt/year and 135 t/d. The lowest values recorded during this period range ~50-60 t/d (**Error! Reference source not found.**), similarly to the total flux of ~53 t/d estimated by Padrón et al., (2008). This indicates that the baseline of the lake CO_2 emission must be around 50 t/d, corresponding to a minimum value occurring during stratified periods. Variations caused by lake overturn periods and possibly the internal activity of the volcano can easily triple or quintuple this value. We have also established a threshold of approximate 170 t/d for "normal" peak degassing during overturn periods. This "normal peak degassing" was defined based on the time series showed on Figure 5A and the fact that from 2015 to 2019 no significant seismo-volcanic activity was detected in the volcano. The values exceeding this limit should probably reveal changes in the volcanic activity.

A comparison between lake-surface area and total CO_2 fluxes for many volcanic lakes around the world is shown in Figure 7-A. Cuicocha presents a low emission when compared with similar area lakes. Figure 7-B shows the total flux normalized for area units (km^2), Cuicocha presents similar degassing to that observed Furnas (Azores) and Monoun lake (Cameroon) (Andrade et al. 2016, and references therein). The CO_2 global emissions for worldwide volcanic lakes have been estimated ~94-104 Mt/year (Burton et al., 2013; Pérez et al., 2011, Werner et al., 2019), which in turn correspond to about 18% of the subaerial volcanic emissions in the world (Burton et al., 2013). Cuicocha CO_2 emissions correspond ~0.01% of the global estimation for volcanic emissions and ~0.05% for volcanic lakes.

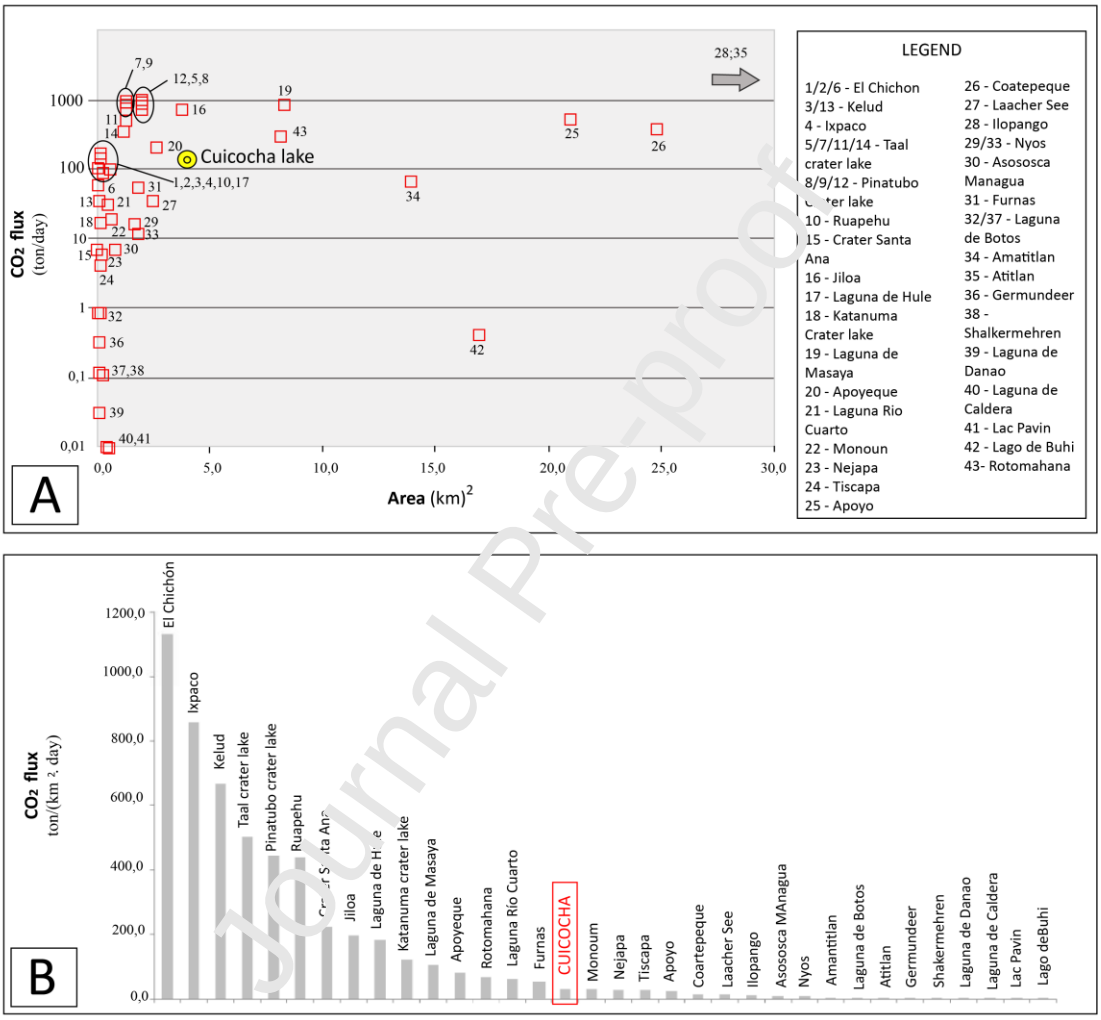

Figure 7.- A) CO_2 flux estimated for various volcanic lakes of the world vs. the surface area of the water bodies. Data from Cuicocha average emission (present work) is shown with yellow dot (Modified from: Andrade et al. 2016, and references therein). B) The same data normalized to the area for all plotted lakes (Modified from: Andrade et al. 2016 to actualize Cuicocha data).

5.5 Implications on Risk and Volcanic Monitoring

After the limnic eruption of 1986 in the lake Nyos (west of Cameroon), which caused ~1700 human casualties and ~3500 livestock losses due to the releasing of more than 1.6 Mt of CO_2 (Fomine, 2011; Kling et al., 1987), the scientific community focused on the evaluation and monitoring of these kind of phenomena. CO_2 can be a dangerous gas, a person should not be exposed more than 15 min to concentrations of 3%, since it can cause several health effects. Lethal concentrations for CO_2 are usually reported above 10% vol. (Viveiros et al., 2016 and references therein). When it is released, as CO_2 gas-cloud has a higher density than the

surrounding air, so it can spread out at ground level causing high risk of CO_2 suffocation in zones with low topographies (D'Alessandro, 2006; Edmonds et al., 2015).

The activity from Cuicocha has always been a concern for those who live or work nearby. The death of 6 people caused by CO_2 inhalation in a small thermal-spa of Tangalí (located 5 km south from CCVC) in January 2015 (Benalcazar, 2015), has been a reminder to the Ecuadorian people about the danger that volcanic gases could pose. Fortunately, previous research in Cuicocha shows that a limnic eruption is not probable to occur (Gunkel et al., 2008). Most of the time, the gas flux is low and overturn periods seem to release major portions of the gas trapped in deep preventing long term accumulation. Additionally, physical and chemical analyses of the water presented by Gunkel et al. (2008) and Gunkel and Beulker, (2009) suggested that there are no high accumulations of CO_2 at deep levels (0,03 l of CO_2/l water).

Diffuse emissions on Cuicocha are relatively low, with an open area and windy Caldera they do not seem to represent an imminent danger. Besides, the lake is part of the "Cotacachi-Cayapas Ecological Reserve", where motorized and no-motorized water-sports are forbidden, also tourists are not allowed to swim. The access to Wolf and Yerovi islets is also restricted, visitors can only enter the lake over touristic boats, operated by the staff of the Municipality of Cotacachi. These actions not only favor the conservation of the natural reserve but also guarantee the safety of people visiting this touristic area. Despite this care, it is recommended to be cautious in those areas characterized by anomalous degassing, especially if changes such as increase in bubbling or changes in water temperature are observed.

Besides, it is noteworthy that the CO_2 being released so far, corresponds mainly to a background level, only two minor anomalous degassing episodes were registered in 2012-2013. The amount of CO_2 released in response to a real volcanic unrest event is still unknown and hence should be considered among the hazards posed by this volcanic lake. Importantly, having established the background CO_2 emissions and their behavior due to seasonal changes in the lake will significantly improve geochemical monitoring allowing to easily recognize potential degassing anomalies in the future.

6.- Conclusions

This work contributes to the existing knowledge of Cuicocha Caldera Lake by providing a long-term analysis of CO_2 diffuse degassing, probably the longest temporal CO_2 series available on a crater lake worldwide. Furthermore, it includes an interpretation of the relationship between carbon dioxide diffuse degassing and the structural scenario of the CCVC.

In the period between 2011-2019, Cuiococha lake has presented CO_2 diffuse emissions ranging ~50-250 t/d. During 8.13 years of periodic surveys, Cuicocha released more than 400 kt of CO_2 with an average rate of ~135 t/d.

Degassing in Cuicocha lake shows a major influence from the lake dynamics. In the period ~Sep-May the climatic conditions favor water stratification, this stratification allows gas storage in the deep layers, causing lower manifestations at surface. During the period ~Jun-Aug, an overturn occurs in the lake and monomictic circulation releases the stored gas to the surface.

Gas emission peaks registered in 2012-2013 are anomalous if compared with other peaks registered afterwards. Considering the anomalous seismicity occurring in the volcano during that period, we consider that the increase in CO_2 flux must be related to deep origin processes affecting the hydrothermal system.

Degassing in Cuicocha lake is controlled by the presence of degassing structures. The proposed location for these structures corresponds to high permeability damage zones, caused by the intersection of ~NE-SW oriented faults, associated with the Billecocha-Hayrapungo system, and ~WNW-ESE oriented minor structures.
Moreover, a baseline in CO_2 degassing has been established for Cuicocha lake; with minimum total fluxes ~50 t/d registered during stratified periods and maximums total fluxes ~170 t/d registered for overturn periods. This baseline will significantly improve geochemical monitoring of the lake.

FUNDING

This research is funded by the Project "Generación de Capacidades para la emisión de alertas tempranas-SENPLADES; the "Convenio de Cooperación Técnica y Científica entre la Escuela Politécnica Nacional y el Gobierno Autónomo Descentralizado Municipal de Santa Ana de Cotacachi"; and research projects obtained by the IG-EPN through SENESCYT and BID.

ACKNOWLEDGEMENTS

We would like to express our gratitude to the IGEPN staff who participated on the field surveys and to the Empresa Pública de Turismo Cotacachi E.p., for providing the boat logistics. Fatima Viveiros, and an anonymous reviewer are kindly acknowledged for their thoughtful comments which improved the manuscript. We also thank Alessandro Aiuppa for the editorial handling.

REFERENCES:

- Almeida, M., 2016. Estudio petrográfico y geoquímico del volcán Cotacachi–provincia de Imbabura (B.S. thesis). Quito, 2016.
- Almeida, M., Bablon, M., Andrade, D., Hidalgo, S., Quidelleur, X., Samaniego, P., 2019. New constraints on the geological and chronological evolution of the Cotacachi-Cuicocha Volcanic Complex (Ecuador), in: 8th International Symposium on Andean Geodynamics (ISAG).
- Alvarado, A., 2012. Néotectonique et cinématique de la déformation continentale en Equateur (PhD Thesis). Université de Grenoble.
- Andrade, C., Viveiros, F., Cruz, J.V., Coutinho, R., Silva, C., 2016. Estimation of the CO_2 flux from Furnas volcanic lake (Sao Miguel, Azores). J. Volcanol. Geotherm. Res. 315, 51–64.
- Andrade, R., Guarderas, M., 2017. Hoja Geológica 1:50 000, Otavalo.
- Arellano, S.R., Hall, M., Samaniego, P., Le Pennec, J.-L., Ruiz, A., Molina, I., Yepes, H., 2008. Degassing patterns of Tungurahua volcano (Ecuador) during the 1999–2006 eruptive period, inferred from remote spectroscopic measurements of SO_2 emissions. J. Volcanol. Geotherm. Res. 176, 151–162.
- Aspden, J.A., Litherland, M., 1992. The geology and Mesozoic collisional history of the Cordillera Real, Ecuador. Tectonophysics 205, 187–204.

- Benalcazar, W., 2015. 6 Personas murieron en un ritual en Otavalo. El Comer.
- Bendix, J., Lauer, W., 1992. Die Niederschlagsjahreszeiten in Ecuador und ihre klimadynamische Interpretation (Rainy seasons in ecuador and their climate-dynamic interpretation). Erdkunde 118–134.
- Bernard, A., Escobar, C.D., Mazot, A., Gutiérrez, R.E., 2004. The acid volcanic lake of Santa Ana volcano, El Salvador. Spec. Pap.-Geol. Soc. Am. 121–134.
- Bernard, B., Andrade, D., 2011. Mapa del volcanismo Cuaternario del Ecuador.
- Bernard, B., Battaglia, J., Proaño, A., Hidalgo, S., Vásconez, F., Hernandez, S., Ruiz, M., 2016. Relationship between volcanic ash fallouts and seismic tremor: quantitative assessment of the 2015 eruptive period at Cotopaxi volcano, Ecuador. Bull. Volcanol. 78, 80.
- Bini, G., Chiodini, G., Lucchetti, C., Moschini, P., Caliro, S., Mollo, S., Selva, J., Tuccimei, P., Galli, G., Bachmann, O., 2020. Deep versus shallow sources of -CO_2 and Rn from a multi-parametric approach: the case of the Nisyros caldera (Aegean Arc, Greece).
- Bourdon, E., Eissen, J.-P., Gutscher, M.-A., Monzier, M., Hall, M.L., Cotten, J., 2003. Magmatic response to early aseismic ridge subduction: the Ecuadorian margin case (South America). Earth Planet. Sci. Lett. 205, 123–138.
- Burton, M.R., Sawyer, G.M., Granieri, D., 2013. Deep carbon emissions from volcanoes. Rev. Mineral. Geochem. 75, 323–354.
- Carapezza, M.L., Granieri, D., 2004. CO_2 soil flux at Vulcano (Italy): comparison between active and passive methods. Appl. Geochem. 19, 73–88.
- Cardellini, C., Chiodini, G., Frondini, F., 2003. Application of stochastic simulation to CO_2 flux from soil: mapping and quantification of gas release. J. Geophys. Res. Solid Earth 108.
- Cardellini, C., Chiodini, G., Frondini, F., Avino, R., Bagnato, E., Caliro, S., Lelli, M., Rosiello, A., 2017. Monitoring diffuse volcanic degassing during volcanic unrests: the case of Campi Flegrei (Italy). Sci. Rep. 7, 1–15.
- Chiodini, G., Cioni, R., Guidi, M., Raco, B., Marini, L., 1998. Soil CO_2 flux measurements in volcanic and geothermal areas. Appl. Geochem. 13, 543–552.
- Chiodini, G., Frondini, F., Cardellini, C., Granieri, D., Marini, L., Ventura, G., 2001. CO_2 degassing and energy release at Solfatara volcano, Campi Flegrei, Italy. J. Geophys. Res. Solid Earth 106, 16213–16221.
- Cordova, A., 2013. Estudio de micro-sismicidad para los proyectos geotérmicos: Chacana y Chachimbiro (B.S. thesis). Quito, 2013.
- Curewitz, D., Karson, J.A., 1997. Structural settings of hydrothermal outflow: fracture permeability maintained by fault propagation and interaction. J. Volcanol. Geotherm. Res. 79, 149–168.
- D'Alessandro, W., 2006. Gas hazard: an often neglected natural risk in volcanic areas. WIT Trans. Ecol. Environ. 89.

- David, M., 1977. Geostatistical ore reserve estimation. Elsevier.
- Deutsch, C.V., Journel, A.G., 1998. GSLib. Geostat. Softw. Libr. User's Guide 369.
- Edmonds, M., Grattan, J., Michnowicz, S., 2015. Volcanic gases: silent killers, in: Observing the Volcano World. Springer, pp. 65–83.
- Ego, F., Sébrier, M., Lavenu, A., Yepes, H., Egues, A., 1996. Quaternary state of stress in the Northern Andes and the restraining bend model for the Ecuadorian Andes. Tectonophysics 259, 101–116.
- Eguez, A., Albán, A., 2017. Mapa Geológico de la República de Ecuador.
- Eguez, A., Alvarado, A., Yepes, H., Machette, M.N., Costa, C., Dart, R.L., Bradley, L.A., 2003. Database and map of Quaternary faults and folds of Ecuador and its offshore regions. US Geol. Surv. Open-File Rep. 3, 289.
- Eguez, A., Yepes, H., 1993. Estudios Sismotectónicos y de peligro sísmico para el proyecto hidroeléctrico Chespí.
- Fischer, T.P., Aiuppa, A., 2020. AGU Centennial Grand Challenge: Volcanoes and Deep Carbon Global CO_2 Emissions From Subaerial Volcanism—Recent Progress and Future Challenges. Geochem. Geophys. Geosystems 21, e2019GC008690.
- Fischer, T.P., Chiodini, G., 2015. Volcanic, Magmatic and Hydrothermal Gases. Elsevier, pp. 779–797. doi:10.1016/B978-0-12-385938-9.00045-6
- Fomine, F.L.M., 2011. The Strange Lake Nyos CO_2 Gas Disaster: Impact and The Displacement and Return of the Affected Communities. Australas. J. Disaster Trauma Stud. ISSN 1174–4707.
- Freymueller, J.T., Kellogg, J.N., Vega, V., 1993. Plate motions in the north Andean region. J. Geophys. Res. Solid Earth 98, 21853–21863.
- Garcia-Aristizabal, A., Kumagai, H., Samaniego, P., Mothes, P., Yepes, H., Monzier, M., 2007. Seismic, petrologic, and geodetic analyses of the 1999 dome-forming eruption of Guagua Pichincha volcano, Ecuador. J. Volcanol. Geotherm. Res. 161, 333–351.
- Gaunt, H.E., Bernard, B., Hidalgo, S., Proaño, A., Wright, H., Mothes, P., Criollo, E., Kueppers, U., 2016. Juvenile magma recognition and eruptive dynamics inferred from the analysis of ash time series: The 2015 reawakening of Cotopaxi volcano. J. Volcanol. Geotherm. Res. 328, 134–146.
- Giammanco, S., Gurrieri, S., Valenza, M., 1998. Anomalous soil CO_2 degassing in relation to faults and eruptive fissures on Mount Etna (Sicily, Italy). Bull. Volcanol. 60, 252–259.
- Graindorge, D., Calahorrano, A., Charvis, P., Collot, J.-Y., Bethoux, N., 2004. Deep structures of the Ecuador convergent margin and the Carnegie Ridge, possible consequence on great earthquakes recurrence interval. Geophys. Res. Lett. 31.
- Guillier, B., Chatelain, J.-L., Jaillard, E., Yepes, H., Poupinet, G., Fels, J.-F., 2001. Seismological evidence on the geometry of the Orogenic System in central-northern Ecuador (South America). Geophys. Res. Lett. 28, 3749–3752.

- Gunkel, G., 2000. Limnology of an equatorial high mountain lake in Ecuador, Lago San Pablo. Limnologica 30, 113–120.
- Gunkel, G., Beulker, C., 2009. Limnology of the Crater Lake Cuicocha, Ecuador, a cold water tropical lake. Int. Rev. Hydrobiol. 94, 103–125.
- Gunkel, G., Beulker, C., Grupe, B., Viteri, F., 2008. Hazards of volcanic lakes: analysis of Lakes Quilotoa and Cuicocha, Ecuador.
- Gunkel, G., Viteri, F., Beulker, C., Grupe, B., 2006. Accumulation of Carbon Dioxide in deep caldera lakes of Ecuador: evaluation and monotpring of possible gas eruptions.
- Gutscher, M.-A., Malavieille, J., Lallemand, S., Collot, J.-Y., 1999. Tectonic segmentation of the North Andean margin: impact of the Carnegie Ridge collision. Earth Planet. Sci. Lett. 168, 255–270.
- Hall, M.L., Beate, B., 1991. El volcanismo plio-cuaternario en los Andes del Ecuador. Estud. Geogr. 4, 5–38.
- Hall, M.L., Samaniego, P., Le Pennec, J.-L., Johnson, J.B., 2008. Ecuadorian Andes volcanism: A review of Late Pliocene to present activity. J. Volcanol. Geotherm. Res. 176, 1–6.
- Hernández, P.A., Notsu, K., Salazar, J.M., Mori, T., Natale, G., Okada, H., Virgili, G., Shimoike, Y., Sato, M., Pérez, N.M., 2001. Carbon dioxide degassing by advective flow from Usu volcano, Japan. Science 292, 83–86.
- Hernández, P.A., Pérez, N.M., Salazar, J.M., Nakai, S., Notsu, K., Wakita, H., 1998. Diffuse emission of carbon dioxide, methane, and helium-3 from Teide Volcano, Tenerife, Canary Islands. Geophys. Res. Lett. 25, 3311–3314.
- Hidalgo, S., Battaglia, J., Arellano, S., Sierra, D., Bernard, B., Parra, R., Kelly, P., Dinger, F., Barrington, C., Samaniego, P., 2018. Evolution of the 2015 Cotopaxi eruption revealed by combined geochemical and seismic observations. Geochem. Geophys. Geosystems 19, 2087–2108.
- Hidalgo, S., Battaglia, J., Arellano, S., Steele, A., Bernard, B., Bourquin, J., Galle, B., Arrais, S., Vásconez, F., 2015. SO_2 degassing at Tungurahua volcano (Ecuador) between 2007 and 2013: transition from continuous to episodic activity. J. Volcanol. Geotherm. Res. 298, 1–14.
- Hidalgo, S., Gerbe, M.C., Martin, H., Samaniego, P., Bourdon, E., 2012. Role of crustal and slab components in the Northern Volcanic Zone of the Andes (Ecuador) constrained by Sr–Nd–O isotopes. Lithos 132, 180–192.
- Hidalgo, S., Palacios, P., Robles, A., Pacheco, D., Batalglia, J., Yuccha, V., Narvaez, D., Hashelle, N., Sonja Storm, Goergouz, C., 2014. Results from CO_2 measurement campaigns at Cuicocha crater lake (Ecuador).
- Hughes, R.A., Pilatasig, L.F., 2002. Cretaceous and Tertiary terrane accretion in the Cordillera Occidental of the Andes of Ecuador. Tectonophysics 345, 29–48.
- IGEPN, 2019. Informe Anual del Complejo Volcánico Cotacachi y Cuicocha – 2019.

- IGEPN, 2018. Informe Anual del Complejo Volcánico Cotacachi y Cuicocha – 2018.
- IGEPN, 2010. Informe Sísmico para el año 2010.
- Inguaggiato, S., Hidalgo, S., Beate, B., Bourquin, J., 2010. Geochemical and isotopic characterization of volcanic and geothermal fluids discharged from the Ecuadorian volcanic arc. Geofluids 10, 525–541.
- Kling, G.W., Clark, M.A., Wagner, G.N., Compton, H.R., Humphrey, A.M., Devine, J.D., Evans, W.C., Lockwood, J.P., Tuttle, M.L., Koenigsberg, E.J., 1987. The 1986 lake Nyos gas disaster in cameroon, west Africa. Science 236, 169–175.
- Lamberti, M.C., Vigide, N., Venturi, S., Agusto, M., Yagupsky, D., Winocur, D., Barcelona, H., Velez, M.L., Cardellini, C., Tassi, F., 2019. Structural architecture releasing deep-sourced carbon dioxide diffuse degassing at the Caviahue–Copahue Volcanic Complex. J. Volcanol. Geotherm. Res. 374, 131–141.
- Lavenu, A., 1995. Geodinámica plio-cuaternaria en los Andes centrales: el Altiplano norte de Bolivia. Rev. Téc. Yacim. Pet. Fisc. Boliv. 16, 79–96.
- Liss, P., Slater, P.G., 1974. Flux of gases across the air-sea interface. Nature 247, 181–184.
- Mardia, K.V., 1972. Statistics of directional data Academic. London.
- Martel, S.J., Boger, W.A., 1998. Geometry and mechanics of secondary fracturing around small three-dimensional faults in granitic rock. J. Geophys. Res. Solid Earth 103, 21299–21314.
- Mazot, A., 2005. CO_2 degassing and fluid geochemistry at Papandayan and Kelud volcanoes. Java Isl. Indones. P'Thesis Bruss. Univ. Libre Brux.
- Mazot, A., Schwandner, F.M., Christenson, B., De Ronde, C.E., Inguaggiato, S., Scott, B., Graham, D., Britten, K., Keeman, J., Tan, K., 2014. CO_2 discharge from the bottom of volcanic Lake Rotomahana, New Zealand. Geochem. Geophys. Geosystems 15, 577–588.
- Mazot, A., Taran, Y., 2009. CO_2 flux from the volcanic lake of El Chichón (Mexico). Geofísica Int. 48, 73–83.
- McGillis, W.R., Wanninkhof, R., 2006. Aqueous CO_2 gradients for air–sea flux estimates. Mar. Chem. 98, 100–108.
- Melián, G., Hernández, P.A., Padrón, E., Pérez, N.M., Barrancos, J., Padilla, G., Dionis, S., Rodríguez, F., Calvo, D., Nolasco, D., 2014. Spatial and temporal variations of diffuse CO_2 degassing at El Hierro volcanic system: relation to the 2011–2012 submarine eruption. J. Geophys. Res. Solid Earth 119, 6976–6991.
- Monzier, M., Robin, C., Samaniego, P., Hall, M.L., Cotten, J., Mothes, P., Arnaud, N., 1999. Sangay volcano, Ecuador: structural development, present activity and petrology. J. Volcanol. Geotherm. Res. 90, 49–79.
- Nocquet, J.-M., Mothes, P., Alvarado, A., 2009. Geodesia, geodinámica y ciclo sísmico en Ecuador. Geol. Geofis. Mar. Terr. Ecuad. 83–95.

- Notsu, K., Sugiyama, K., Hosoe, M., Uemura, A., Shimoike, Y., Tsunomori, F., Sumino, H., Yamamoto, J., Mori, T., Hernández, P.A., 2005. Diffuse CO_2 efflux from Iwojima volcano, Izu-Ogasawara arc, Japan. J. Volcanol. Geotherm. Res. 139, 147–161.
- O'leary, D.W., Friedman, J.D., Pohn, H.A., 1976. Lineament, linear, lineation: some proposed new standards for old terms. Geol. Soc. Am. Bull. 87, 1463–1469.
- Padrón, E., Hernández, P.A., Toulkeridis, T., Pérez, N.M., Marrero, R., Melián, G., Virgili, G., Notsu, K., 2008. Diffuse CO_2 emission rate from Pululahua and the lake-filled Cuicocha calderas, Ecuador. J. Volcanol. Geotherm. Res. 176, 163–169.
- Papale, P., Rosi, M., 1993. A case of no-wind plinian fallout at Pululagua caldera (Ecuador): implications for models of clast dispersal. Bull. Volcanol. 55, 523–535.
- Parkinson, K.J., 1981. An improved method for measuring soil respiration in the field. J. Appl. Ecol. 221–228.
- Pennington, W.D., 1981. Subduction of the eastern Panama Basin and seismotectonics of northwestern South America. J. Geophys. Res. Solid Earth 86, 10753–10770.
- Pérez, N.M., Hernández, P.A., Padilla, G., Nolasco, D., Barrancos, J., Melían, G., Padrón, E., Dionis, S., Calvo, D., Rodríguez, F., 2011. Global CO_2 emission from volcanic lakes. Geology 39, 235–238.
- Pérez, N.M., Hernández, P.A., Padrón, E., Cartagena, R., Olmos, R., Barahona, F., Melián, G., Salazar, P., López, D.L., 2006. Anomalous diffuse CO_2 emission prior to the January 2002 short-term unrest at San Miguel Volcano, El Salvador, Central America. Pure Appl. Geophys. 163, 883–896.
- Pidgen, A., 2014. Cuicocha Volcano, Ecuador: Reconstruction of major explosive phases throught investigation of associated pyroclastic deposits.
- Pratt, W.T., Duque, P., Ponce, M., 2005. An autochthonous geological model for the eastern Andes of Ecuador. Tectonophysics 399, 251–278.
- QGIS Development Team, 2015. QGIS Geographic Information System. Open Source Geospatial Foundation Project.
- Rautman, C.A., Istok, J.D., 1996. Probabilistic assessment of ground-water contamination: 1. Geostatistical framework. Groundwater 34, 899–909.
- Rogie, J.D., Kerrick, D.M., Sorey, M.L., Chiodini, G., Galloway, D.L., 2001. Dynamics of carbon dioxide emission at Mammoth Mountain, California. Earth Planet. Sci. Lett. 188, 535–541.
- Ruiz, A.G., Samaniego, P., von Hillebrandt-Andrade, C., Hall, M.L., Ruiz, M.C., Mothes, P.A., Macias, C.A., 2013. Multiparameter Monitoring Techniques for Reducing Volcanic Risk from Cuicocha Crater Lake, Ecuador. AGUSM 2013, V44A–08.
- Samaniego, P., Barba, D., Robin, C., Fornari, M., Bernard, B., 2012. Eruptive history of Chimborazo volcano (Ecuador): A large, ice-capped and hazardous compound volcano in the Northern Andes. J. Volcanol. Geotherm. Res. 221, 33–51.

- Samaniego, P., Eissen, J.-P., Le Pennec, J.-L., Robin, C., Hall, M.L., Mothes, P., Chavrit, D., Cotten, J., 2008. Pre-eruptive physical conditions of El Reventador volcano (Ecuador) inferred from the petrology of the 2002 and 2004–05 eruptions. J. Volcanol. Geotherm. Res. 176, 82–93.
- Samaniego, P., Monzier, M., Eissen, J.-P., Bourdon, E., Robin, C., Hall, M.L., Martin, H., 2002. Caracterización Geoquímica del Arco Volcánico Ecuatoriano. Quintas Jornadas en Ciencias de la Tierra., Quito, pp. 27-29.
- Sibson, R.H., Rowland, J.V., 2003. Stress, fluid pressure and structural permeability in seismogenic crust, North Island, New Zealand. Geophys. J. Int. 154, 584–594.
- Sinclair, A.J., 1974. Selection of threshold values in geochemical data using probability graphs. J. Geochem. Explor. 3, 129–149.
- Soulas, J.P., 1991. Neotectónica y tectónica activa en Venezuela y regiones vecinas.
- Stern, C.R., 2004. Active Andean volcanism: its geologic and tectonic setting. Rev. Geológica Chile 31, 161–206.
- Sugisaki, R., Ido, M., Takeda, H., Isobe, Y., Hayashi, Y., Nakamura, N., Satake, H., Mizutani, Y., 1983. Origin of hydrogen and carbon dioxide in fault gases and its relation to fault activity. J. Geol. 91, 239–258.
- Tennant, C.B., White, M.L., 1959. Study of the distribution of some geochemical data. Econ. Geol. 54, 1281–1290.
- Tibaldi, A., 2005. Volcanism in compressional tectonic settings: Is it possible? Geophys. Res. Lett. 32.
- Trauth, M.H., Gebbers, R., Marwan, N., Sillmann, E., 2007. MATLAB recipes for earth sciences. Springer.
- Ujueta, G., 2001. Lineamientos de Dirección NO-SE y NNE-SSO a NE-SO en el Centro Occidente Colombiano y en el Ecuador. Geol. Colomb. 26, 5–27.
- Vallejo, C., Winkler, W., Spiking, R.A., Luzieux, L., Heller, F., Bussy, F., 2009. Mode and timing of terrane accretion in theforearc of the Andes in Ecuador. Backbone Am. Shallow Subduction Plateau Uplift Ridge Terrane Collis. 204, 197.
- Viveiros, F., Cardellini, C., Ferreira, T., Caliro, S., Chiodini, G., Silva, C., 2010. Soil CO_2 emissions at Furnas volcano, São Miguel Island, Azores archipelago: Volcano monitoring perspectives, geomorphologic studies, and land use planning application. J. Geophys. Res. Solid Earth 115.
- Viveiros, F., Chiodini, G., Cardellini, C., Caliro, S., Zanon, V., Silva, C., Rizzo, A.L., Hipólito, A., Moreno, L., 2020. Deep CO_2 emitted at Furnas do Enxofre geothermal area (Terceira Island, Azores archipelago). An approach for determining CO_2 sources and total emissions using carbon isotopic data. J. Volcanol. Geotherm. Res. 401, 106968.
- Viveiros, F., Gaspar, J.L., Ferreira, T., Silva, C., 2016. Hazardous indoor CO_2 concentrations in volcanic environments. Environ. Pollut. 214, 776–786.

- Von Hillebrant, C., 1989. Estudio geovolcanológico del Complejo Volcánico Cuicocha-Cotacachi y sus aplicaciones. Provincia de Imbabura. Unpubl. Thesis Esc. Politécnica Nac. Quito Ecuad.
- Werner, C., Fischer, T.P., Aiuppa, A., Edmonds, M., Cardellini, C., Carn, S., Chiodini, G., Cottrell, E., Burton, M., Shinohara, H., 2019. Carbon Dioxide Emissions from Subaerial Volcanic Regions, in: Deep Carbon Past to Present. Cambridge University Press.
- West Systems, 2019. Portable diffuse flux meter Handbook 9,1, 104.
- Woodsworth, G.J., 1971. A geochemical drainage survey and its implications for metallogenesis, central Coast Mountains, British Columbia. Econ. Geol. 66, 1104–1120.
- Yepes, H., Audin, L., Alvarado, A., Beauval, C., Aguilar, J., Font, Y., Cotton, F., 2016. A new view for the geodynamics of Ecuador: Implication in seismogenic source definition and seismic hazard assessment. Tectonics 35, 1249–1279.

Table 1.- Summary statistics of diffuse degassing surveys 2011-2019. Statistical parameters for the results obtained via SGS and GSA. The partitioned lognormal populations interpreted as "high-flow" have been remarked with red and "low –flow" have been remarked in blue.

		Max.	Min.	Mean	Std. Dev.	FLUX SGS	Lognormal Populations												FLUX GSA		Difference Between methods
							A			B			C			D					
Survey Date	# of Points	(g/m^2/day)				t/d	Mean	90% Conf. Inter.	%	Mean	90% Conf. Interval	%	Mean	90% Conf. Interval	%	Mean	90% Conf. Interval	%	Total	(90% conf)	%
16/5/2019	107	48.40	3.12	17.56	8.37	69.34	42.39	36.91 - 56.19	4	28.21	28.05 - 28.47	14	15.58	14.69 - 16.72	75	4.18	3.63 - 5.50	7	69.72	65.97 - 75.82	0.3
30/1/2019	108	313.00	5.98	30.61	35.53	116.86	72.75	69.60 - 80.19	4	35.44	32.71 - 39.44	46	16.47	15.27 - 18.23	44	13.36	8.50 - 37.63	6	107.85	99.15 - 125.14	4.0
9/10/2018	110	76.65	2.55	16.20	10.63	64.02	72.00	62.69 - 95.43	3	22.60	21.62 - 24.03	19	13.85	12.70 - 15.43	63	9.40	8.09 - 11.76	15	65.64	60.15 - 74.84	1.3
26/9/2018	105	159.37	6.31	45.30	31.87	175.08	114.88	74.37 - 308.42	6	80.65	73.45 - 91.98	25	29.96	28.17 - 32.37	59	13.21	9.46 - 26.47	10	182.23	159.82 - 250.24	2.0
30/5/2018	108	89.32	2.86	28.42	17.80	115.65	54.55	40.63 - 102.27	7	42.79	40.04 - 46.82	39	16.96	15.32 - 19.4[illegible]	[illegible]4	4.64	3.96 - 6.26	10	112.50	101.28 - 136.94	1.4
28/2/2018	119	88.53	1.33	16.38	11.82	69.98	46.99	31.40 - 104.60	8	27.55	27.47 - 27.73	4	16.85	16.[illegible]0 - 17.[illegible]4	63	5.88	5.26 - 6.87	25	67.05	59.37 - 89.02	2.1
28/11/2017	110	103.18	2.46	21.80	12.81	87.05	80.46	61.95 - 139.78	3	39.91	38.93 - 42.20	6	19.77	[illegible]3.49 - 21.45	86	5.93	5.53 - 6.87	5	87.46	80.59 - 100.97	0.2
16/8/2017	128	156.90	7.59	42.51	27.20	173.03	158.49	147.75 - 183.81	2	43.74	39.8[illegible] - 4[illegible]14	[illegible]8	15.87	15.70 - 16.24	7	7.94	6.67 - 11.36	2	171.59	156.81 - 192.98	0.4
21/4/2017	104	218.20	0.69	26.55	26.86	105.20	77.09	62.05 - 114.27	9	27.63	26.1[illegible] - 29.70	42	16.44	14.33 - 19.76	43	3.89	2.41 - 11.88	6	102.27	90.47 - 126.49	1.4
28/12/2016	110	160.20	0.91	13.29	15.55	51.78	19.18	18.03 - 21.73	8	1[illegible].85	12.62 - 15.57	70	5.38	5.25 - 5.69	6	4.45	3.10 - 8.37	16	48.53	43.86 - 56.65	3.2
19/9/2016	117	119.99	2.46	33.88	19.19	134.15	53.87	49.99 - 59.77	[illegible]0	[illegible]9.[illegible]	37.96 - 41.03	35	23.77	21.08 - 27.96	35	5.33	4.70 - 6.52	10	132.05	123.19 - 145.41	0.8
31/3/2015	85	377.34	4.52	31.39	42.22	110.82	58.43	49.81 - 7[illegible].82	10	27.63	26.32 - 29.33	67	13.94	13.23 - 15.02	19	5.16	4.81 - 5.99	4	107.65	100.19 - 121.19	1.4
20/3/2014	92	121.57	3.54	30.51	15.94	119.63	5[illegible]56	37.[illegible] - [illegible]5.17	8	41.43	39.23 - 44.62	32	22.98	21.86 - 24.44	55.5	5.89	3.81 - 15.80	4.5	122.50	110.14 - 165.26	1.2
18/9/2013	103	184.93	4.99	57.34	26.10	229.36	94.91	88.50 - 105.10	19	50.89	48.09 - 54.55	74	21.90	21.66 - 22.46	4	12.40	6.47 - 62.93	3	225.28	211.52 - 249.76	0.9
22/5/2013	112	80.39	1.71	13.91	10.56	52.53	20.61	19.70 - 21.94	24	12.86	12.37 - 13.54	38	8.16	8.01 - 8.38	29	3.80	3.02 - 6.01	9	49.62	47.57 - 52.95	2.8
19/9/2012	110	147.62	2.82	64.02	28.62	254.74				74.78	71.33 - 79.19	69	45.30	34.97 - 67.18	31				259.72	237.64 - 298.60	1.0
6/6/2012	110	303.20	4.49	64.37	36.08	249.77	107.61	105.16 - 111.40	14	72.92	71.28 - 75.09	39	46.69	44.17 - 50.25	34	22.67	17.99 - 32.80	13	246.61	236.92 - 262.05	0.6
6/3/2012	105	631.40	3.20	63.96	65.14	248.00	92.60	85.94 - 102.33	45	44.77	44.22 - 45.62	20	29.33	27.66 - 31.79	29	12.06	6.41 - 57.67	6	236.83	221.27 - 268.46	2.3
7/12/2011	97	478.87	2.66	46.57	53.30	163.92	74.15	74.07 - 74.26	40	28.95	23.92 - 38.30	30	15.39	14.38 - 16.99	20	8.94	5.96 - 21.51	10	167.44	159.36 - 184.94	1.1
31/3/2011	84	112.68	2.74	31.73	18.17	116.47	87.47	83.67 - 96.41	5	52.54	52.00 - 53.77	7	27.92	26.09 - 30.33	84	7.19	3.49 - 46.65	4	125.80	118.23 - 142.16	3.8

AUTHOR'S CONTRIBUTIONS

- Daniel Sierra.- participated on the surveys, data processing, elaboration of the figures and writing of the manuscript.
- Silvana Hidalgo.- participated on the funding acquisition, the field surveys, the discussion and made a critical review of the manuscript.
- Marco Almeida.- participated on the field surveys, helped with the discussion made a critical review of the manuscript.
- Nicolas Vigide.- participated on the data processing, discussion and writing of the manuscript.
- María Clara Lamberti.- participated the discussion and the corrections of the manuscript.
- Antonio Proaño.- participated on the surveys and helped in the correction of the manuscript.
- Diego Narvaez.- participated on the surveys.

Declaration of interests

☒ The authors declare that they have no known competing financial interests or personal relationships that could have appeared to influence the work reported in this paper.

☐The authors declare the following financial interests/personal relationships which may be considered as potential competing interests:

Highlights

- Diffuse degassing monitoring is periodically performed at CCVC since 2011.
- The Cuicocha Caldera Lake releases ~135 tons of diffuse CO_2 per day.
- The lake dynamics greatly influences the CO2 degassing of Cuicocha Caldera.
- Long term monitoring permitted the identification of anomalous degassing episodes in 2012-2013.
- Areas of high structural damage constitute favorable pathways for fluids flow.

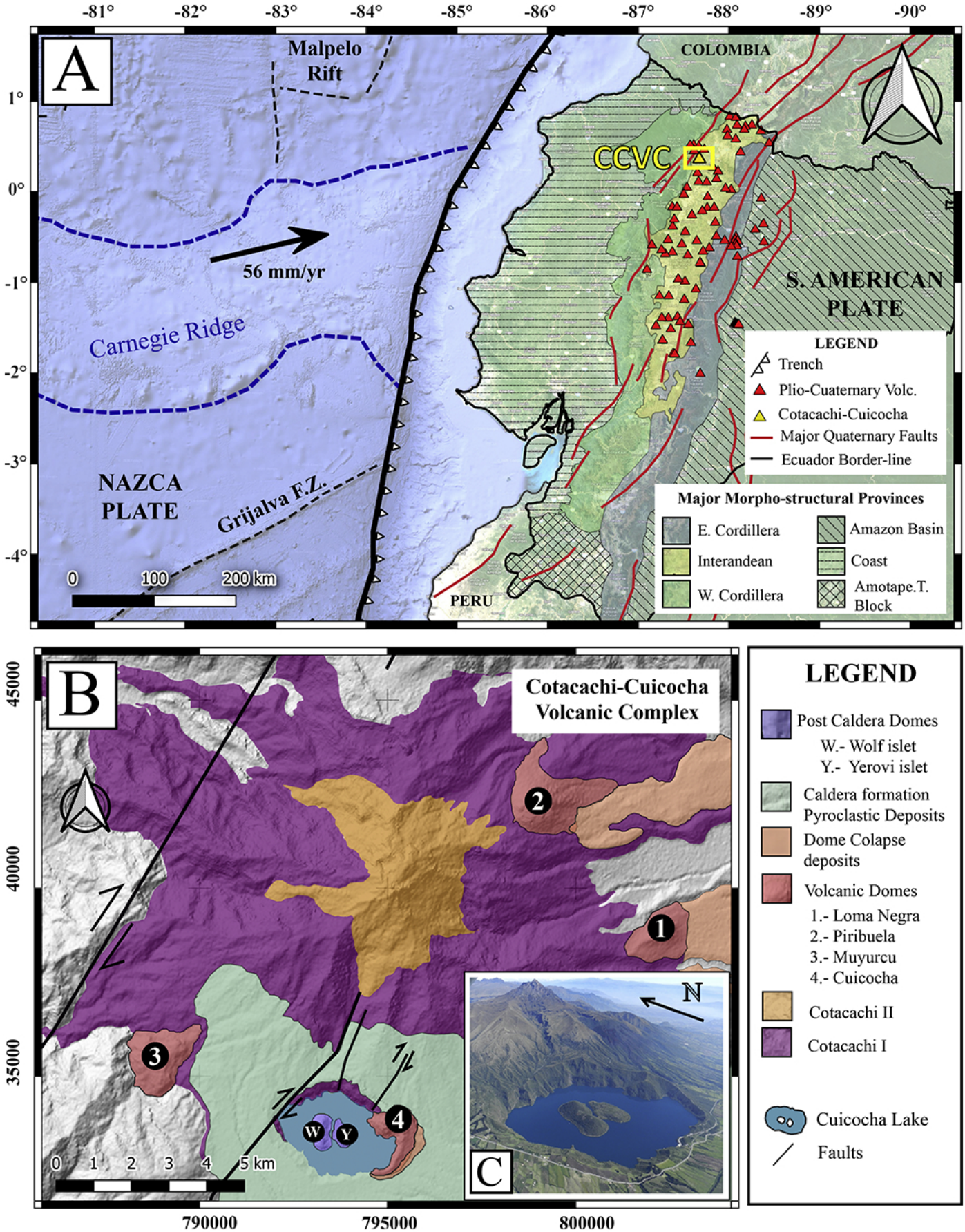
A
Malpelo Rift
COLOMBIA
CCVC
56 mm/yr
Carnegie Ridge
S. AMERICAN PLATE
NAZCA PLATE
Grijalva F.Z.
PERU
0 100 200 km
LEGEND
Trench
Plio-Cuaternary Volc.
Cotacachi-Cuicocha
Major Quaternary Faults
Ecuador Border-line
Major Morpho-structural Provinces
E. Cordillera
Interandean
W. Cordillera
Amazon Basin
Coast
Amotape.T. Block
B
Cotacachi-Cuicocha Volcanic Complex
0 1 2 3 4 5 km
W
Y
C
N
LEGEND
Post Caldera Domes
W.- Wolf islet
Y.- Yerovi islet
Caldera formation Pyroclastic Deposits
Dome Colapse deposits
Volcanic Domes
1.- Loma Negra
2.- Piribuela
3.- Muyurcu
4.- Cuicocha
Cotacachi II
Cotacachi I
Cuicocha Lake
Faults

Figure 1

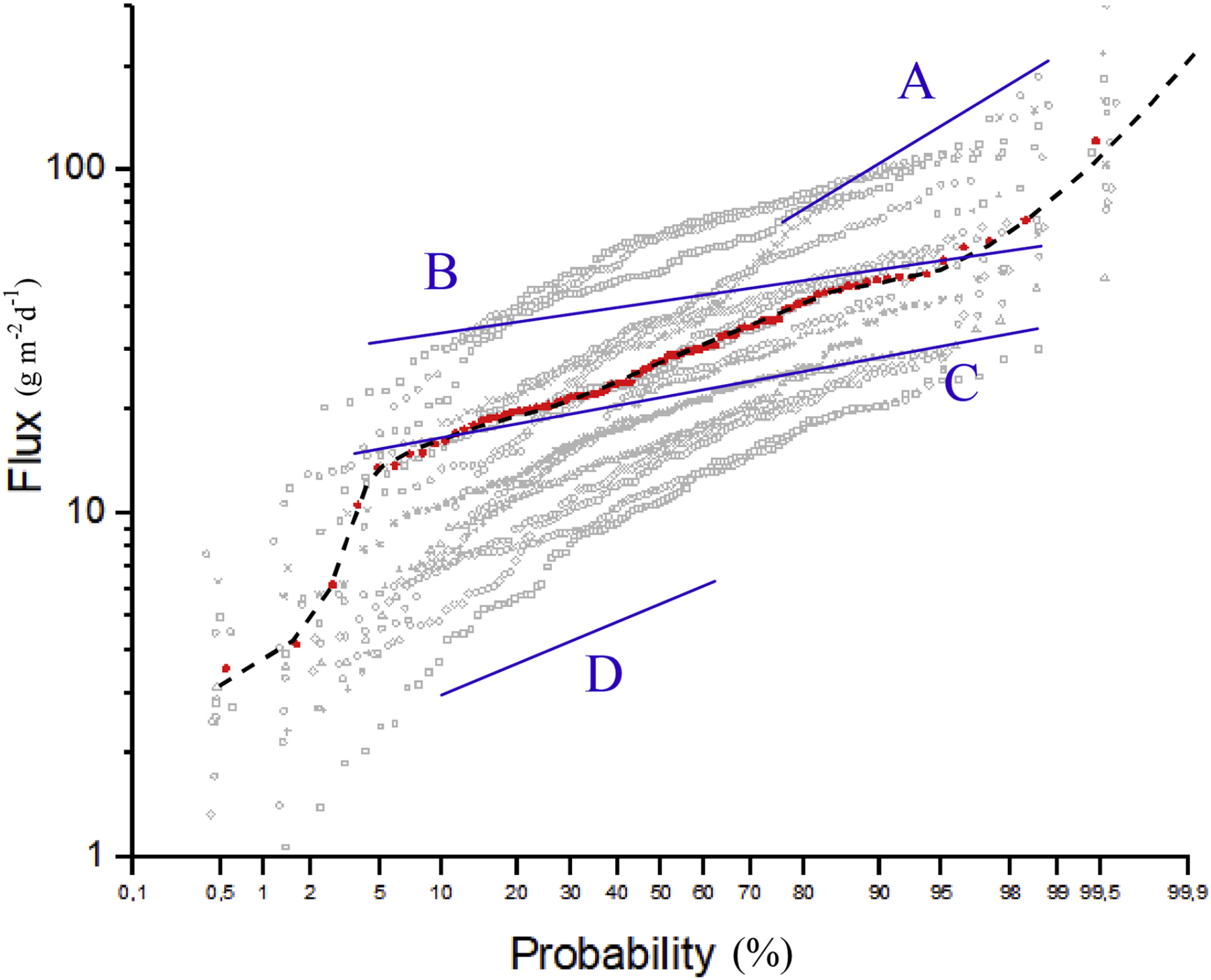
A
B
C
D
100
10
1
Flux (g m-2 d-1)
0,1
0,5
1
2
5
10
20
30
40
50
60
70
80
90
95
98
99
99,5
99,9
Probability (%)

Figure 2

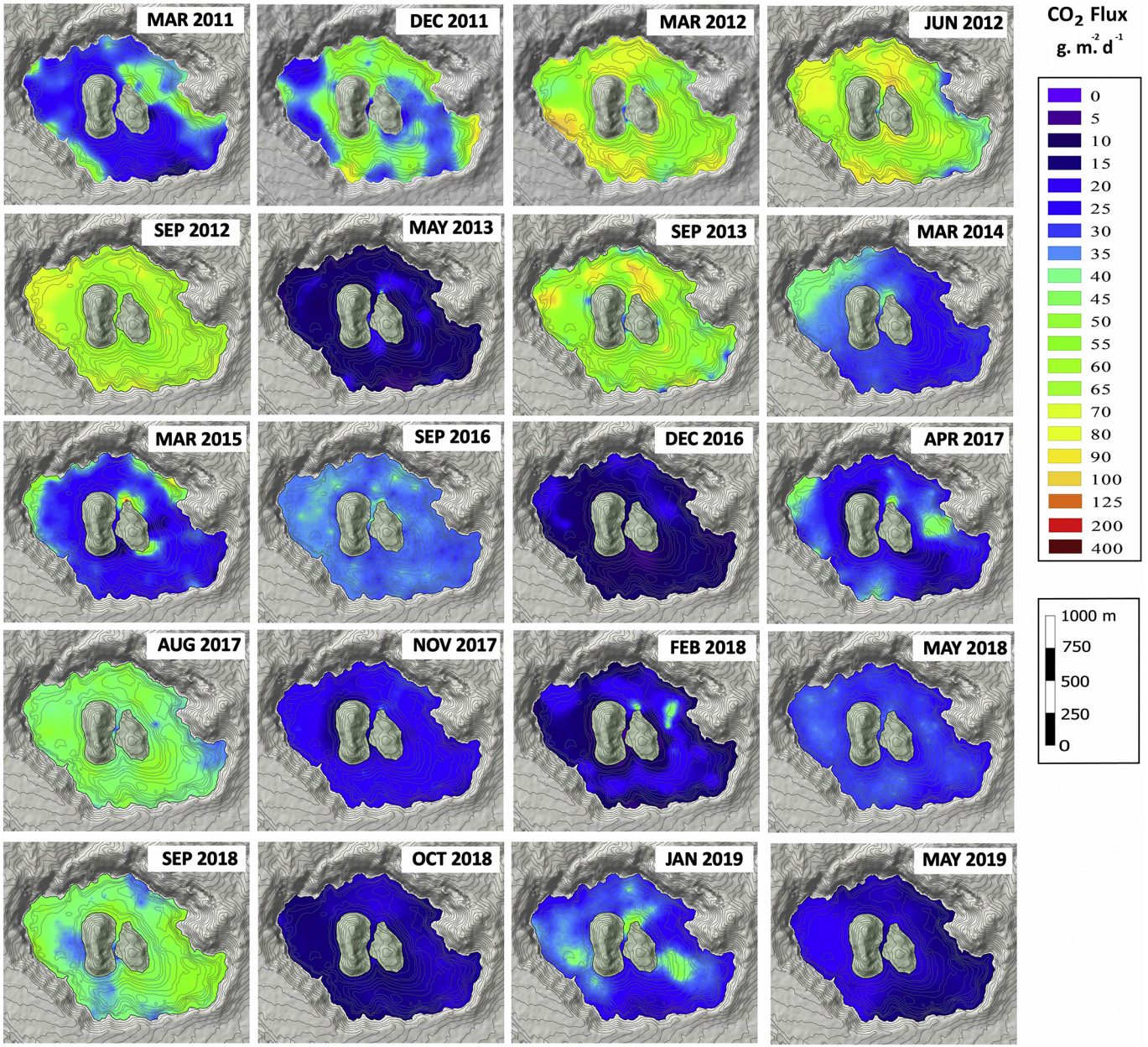
MAR 2011
DEC 2011
MAR 2012
JUN 2012
SEP 2012
MAY 2013
SEP 2013
MAR 2014
MAR 2015
SEP 2016
DEC 2016
APR 2017
AUG 2017
NOV 2017
FEB 2018
MAY 2018
SEP 2018
OCT 2018
JAN 2019
MAY 2019
CO2 Flux
g. m-2 d-1
0
5
10
15
20
25
30
35
40
45
50
55
60
65
70
80
90
100
125
200
400
1000 m
750
500
250
0

Figure 3

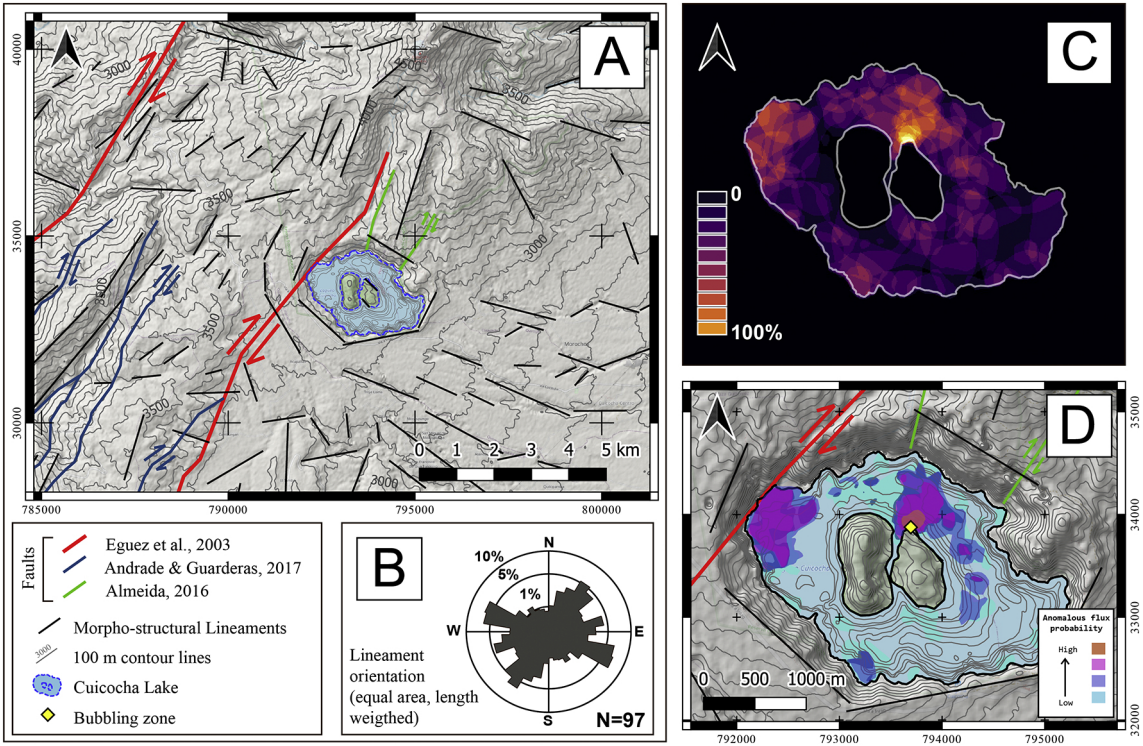
A
B
C
D
0 1 2 3 4 5 km
785000
790000
795000
800000
40000
35000
30000
Faults
Eguez et al., 2003
Andrade & Guarderas, 2017
Almeida, 2016
Morpho-structural Lineaments
100 m contour lines
Cuicocha Lake
Bubbling zone
Lineament orientation (equal area, length weigthed)
N
E
S
W
10%
5%
1%
N=97
0
100%
0 500 1000 m
Anomalous flux probability
High
Low
792000
793000
794000
795000
35000
34000
33000
32000

Figure 4

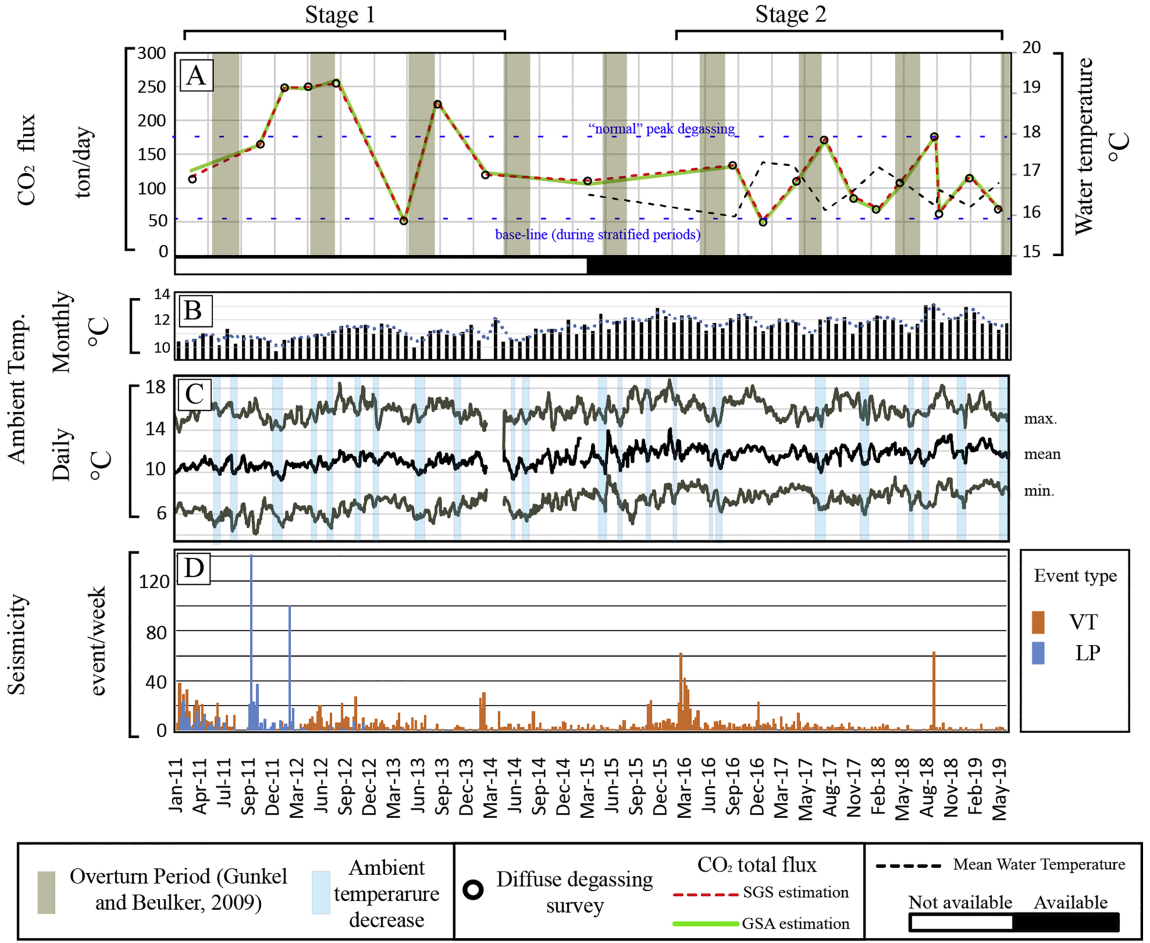
Stage 1
Stage 2
A
B
C
D
CO_2 flux
ton/day
Water temperature
°C
"normal" peak degassing
base-line (during stratified periods)
Ambient Temp.
Monthly
Daily
°C
max.
mean
min.
Seismicity
event/week
Event type
VT
LP
Jan-11
Apr-11
Jul-11
Sep-11
Dec-11
Mar-12
Jun-12
Sep-12
Dec-12
Mar-13
Jun-13
Sep-13
Dec-13
Mar-14
Jun-14
Sep-14
Dec-14
Mar-15
Jun-15
Sep-15
Dec-15
Mar-16
Jun-16
Sep-16
Dec-16
Mar-17
May-17
Aug-17
Nov-17
Feb-18
May-18
Aug-18
Nov-18
Feb-19
May-19
Overturn Period (Gunkel and Beulker, 2009)
Ambient temperarure decrease
Diffuse degassing survey
CO_2 total flux
SGS estimation
GSA estimation
Mean Water Temperature
Not available
Available

Figure 5

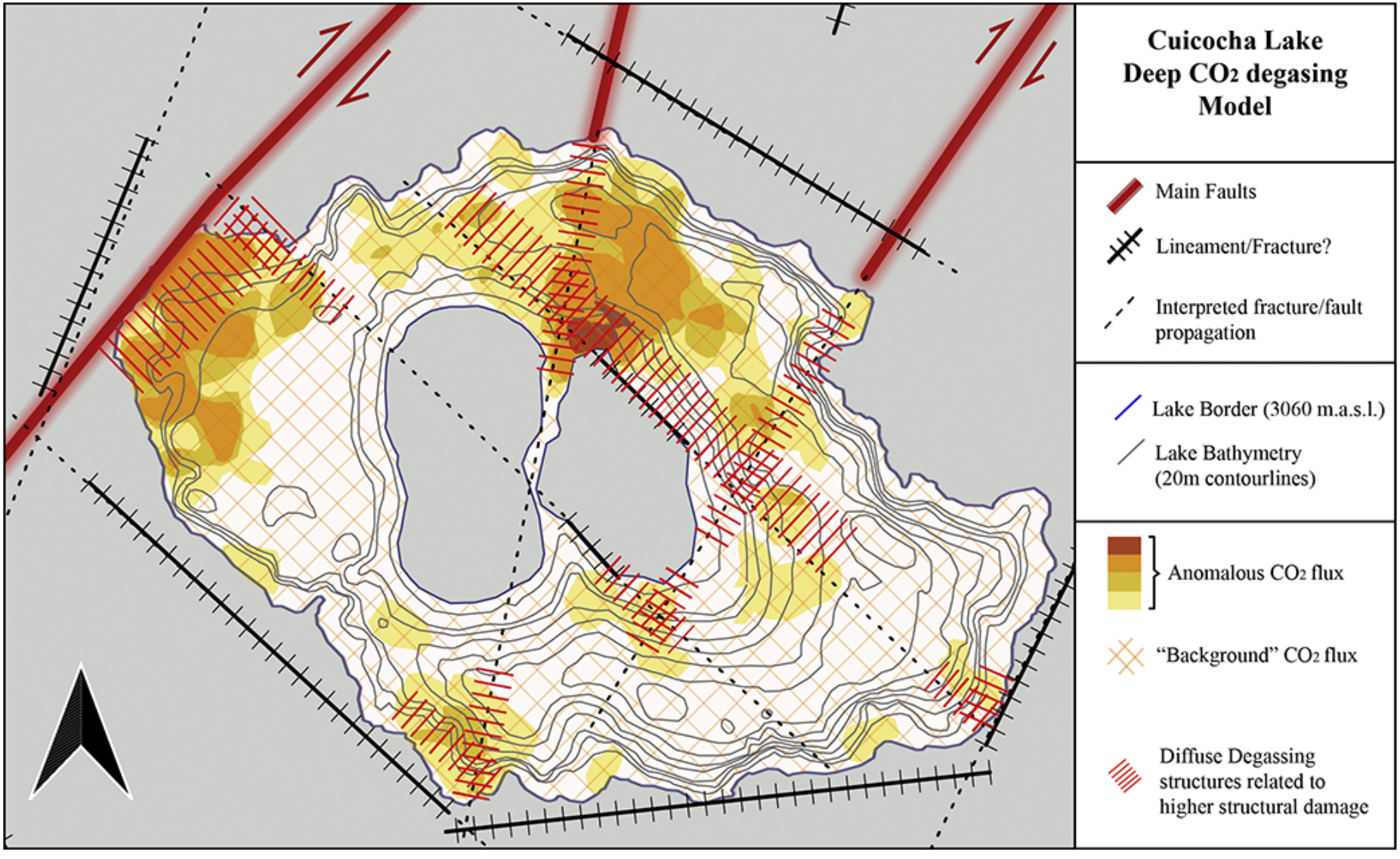
Cuicocha Lake
Deep CO2 degasing
Model
Main Faults
Lineament/Fracture?
Interpreted fracture/fault propagation
Lake Border (3060 m.a.s.l.)
Lake Bathymetry (20m contourlines)
Anomalous CO2 flux
"Background" CO2 flux
Diffuse Degassing structures related to higher structural damage

Figure 6

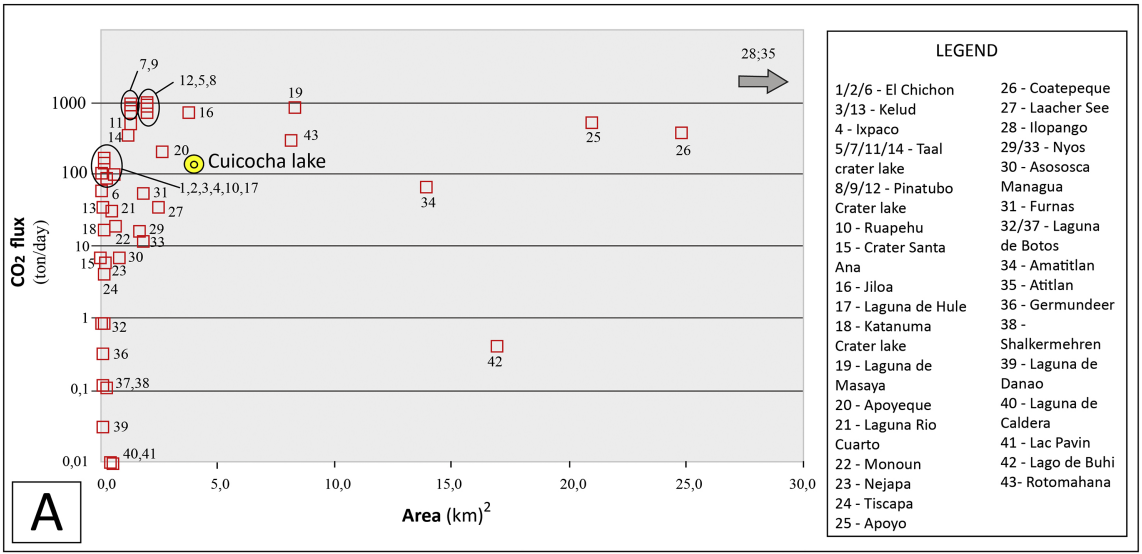
A
CO2 flux
(ton/day)
Area (km)2
Cuicocha lake
28;35
7,9
12,5,8
19
16
11
14
20
43
25
26
1,2,3,4,10,17
6
31
13
21
27
34
18
29
22
33
10
15
30
23
24
32
36
42
37,38
39
40,41
1000
100
10
1
0,1
0,01
0,0
5,0
10,0
15,0
20,0
25,0
30,0
LEGEND
1/2/6 - El Chichon
3/13 - Kelud
4 - Ixpaco
5/7/11/14 - Taal crater lake
8/9/12 - Pinatubo Crater lake
10 - Ruapehu
15 - Crater Santa Ana
16 - Jiloa
17 - Laguna de Hule
18 - Katanuma Crater lake
19 - Laguna de Masaya
20 - Apoyeque
21 - Laguna Rio Cuarto
22 - Monoun
23 - Nejapa
24 - Tiscapa
25 - Apoyo
26 - Coatepeque
27 - Laacher See
28 - Ilopango
29/33 - Nyos
30 - Asososca Managua
31 - Furnas
32/37 - Laguna de Botos
34 - Amatitlan
35 - Atitlan
36 - Germundeer
38 - Shalkermehren
39 - Laguna de Danao
40 - Laguna de Caldera
41 - Lac Pavin
42 - Lago de Buhi
43- Rotomahana

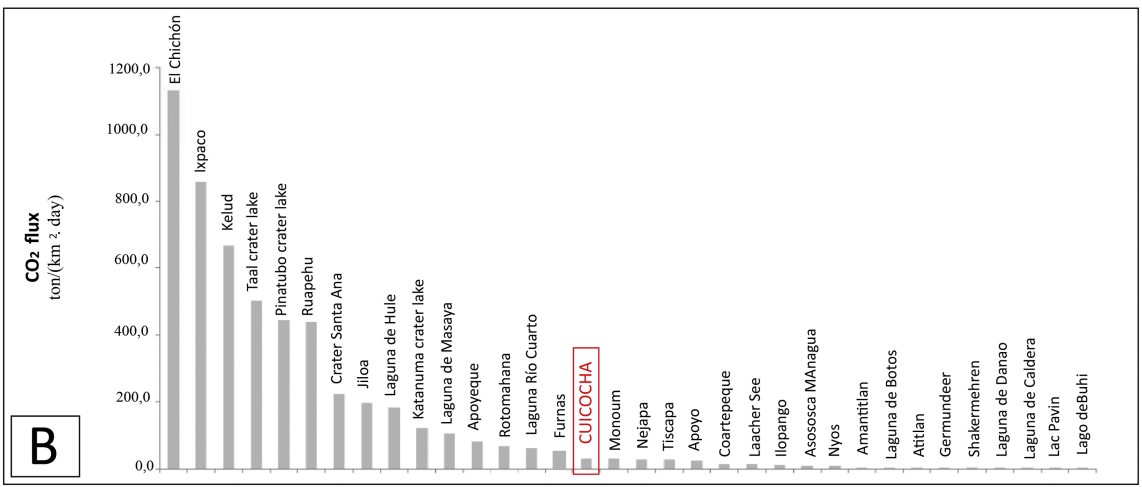
B
CO2 flux
ton/(km 2. day)
1200,0
1000,0
800,0
600,0
400,0
200,0
0,0
El Chichón
Ixpaco
Kelud
Taal crater lake
Pinatubo crater lake
Ruapehu
Crater Santa Ana
Jiloa
Laguna de Hule
Katanuma crater lake
Laguna de Masaya
Apoyeque
Rotomahana
Laguna Río Cuarto
Furnas
CUICOCHA
Monoum
Nejapa
Tiscapa
Apoyo
Coartepeque
Laacher See
Ilopango
Asososca MAnagua
Nyos
Amantitlan
Laguna de Botos
Atitlan
Germundeer
Shakermehren
Laguna de Danao
Laguna de Caldera
Lac Pavin
Lago deBuhi

Figure 7